A PROJECT REPORT ON

Numerical and Experimental Analysis of Jet Impingement Cooling on Hot Flat Surfaces

In partial fulfillment of the requirements for the degree of

B.Tech in Mechanical Engineering

By

HARDIK DAVE

SURESH KUMAR LOHAR

RAHUL KUMAR YADAV

M. AZMAT ALAM

DEPARTMENT OF MECHANICAL ENGINEERING

COLLEGE OF TECHNOLOGY AND ENGINERRING UDAIPUR

MAHARANA PRATAP UNIVERSITY OF AGRICULTURE AND TECHNOLOGY UDAIPUR

Session: 2019-2020

CTAE UDAIPUR

DEPARTMENT OF MECHANICAL ENGG.

A PROJECT REPORT ON

Numerical and Experimental Analysis of Jet Impingement Cooling on Hot Flat Surfaces

In partial fulfillment of the requirements for the degree of

B.Tech in Mechanical Engineering

Session: 2016-2020

Guided By:

Dr. CHITRANJAN AGARWAL

Assistant Professor

Dept. of Mech. Engg.

Submitted by

HARDIK DAVE

SURESH KUMAR LOHAR

RAHUL KUMAR YADAV

M. AZMAT ALAM

CERTIFICATE

This is certify that the project report titled - “**Numerical Analysis of Jet Impingement Cooling on Hot Flat Surfaces”** has been submitted in partial fulfillment of the requirement for the award of degree of Bachelor of Technology in Mechanical Engineering by **HARDIK DAVE** and team **Suresh Kumar Lohar, Rahul Kumar Yadav, M.Azmat Alam** of B.Tech Final year for the academic year 2019-2020.

Approved

PROJECT ADVISOR : Dr. CHITRANJAN AGARWAL

HEAD OF DEPARTMENT : Dr. S. JINDAL

ANKNOWLDGEMENT

We wish to express our sincere gratitude to Dr. Chitranjan Agarwal (Assistant Professor, Mechanical Department) for his invaluable suggestions and guidance throughout our work at the College of Technology And Engineering, Udaipur. The Eager involvement on his part in our dissertation work at every step has been encouraging.

We heartily thank him for his wonderful guidance throughout the project work. He always guided us through the difficulties and made us understand the concept needed for the project his experimental and theoretical know-how was indeed very helpful.

Without his timely help and advice it would not have been possible for us to complete this project.

We also thankful to all the faculty member of the department especially to Mr. Garilalji and Mr. Kuaka ram sir of their kind help.

HARDIK DAVE

SURESH KUMAR LOHAR

RAHUL KUMAR YADAV

M. AZMAT ALAM

Table of Contents

LIST OF FIGURES

LIST OF TABLE

NOMENCLATURE

c : specific heat, kJ kg /K

Re : Reynolds number

d : jet diameter, m

k : thermal conductivity, W/m. K

q : surface heat flux, W/m^2

r : radial distance from the stagnation point, m

T : temperature, °C

T_w : surface temperature within wetted surface, °C

ΔT_{sat} : wall super heat temperature, $(T_i - T_{sat})$, °C

z/d : dimensionless nozzle exit to test surface spacing

Greek Symbols

ρ : density, kg/m^3

υ : kinematic viscosity of water, $m^{2/}$ s

ε : dissipation rate

α : thermal diffusivity, m^2 /s

ABSTRACT

In this study, a numerical method for simulation of flow boiling subcooled jet on a hot surface of steel and aluminum with initial temperature of 773K has been presented. Volume Fraction (VOF) has been used to simulate boiling heat transfer and investigate the quenching phenomenon. The effect of fluid velocity on wet zone propagation, cooling rate and maximum heat flux has been investigated. The investigation is made up for stagnation point to 20 mm downstream location above and below of the stagnation point. Water flow is regulated to maintain the jet Reynolds number in the range of 3000–13,000. It has been observed that maximum surface heat flux is highest for the stagnation point and reduces monotonically for the downstream spatial locations. A comparative study between steel and aluminum has been done. Also the effect of Hardness of water on jet impingement has been carried out by flow visualization.

Keywords: Jet Impingement, Critical Heat flux, wetting front

CHAPTER 1

INTRODUCTION:

Jet impingement cooling is being used in many industrial and engineering applications due to their higher heat removal rate. Because of the attractiveness of jet impingement cooling for high heat flux applications, it is widely used in various industrial processes, namely processing of steel and glasses, cooling of gas turbine blades (Bunker and Metzger, 1990), cooling of IC engine by oil jet (Agarwal and Varghese, 2006; Agarwal et al., 2011), and most recently cooling of various components of electronic devices.

Cooling of Gas turbine blades and components:

Evolution of cooling system over a period of time in gas turbine as shown in the figure1.1

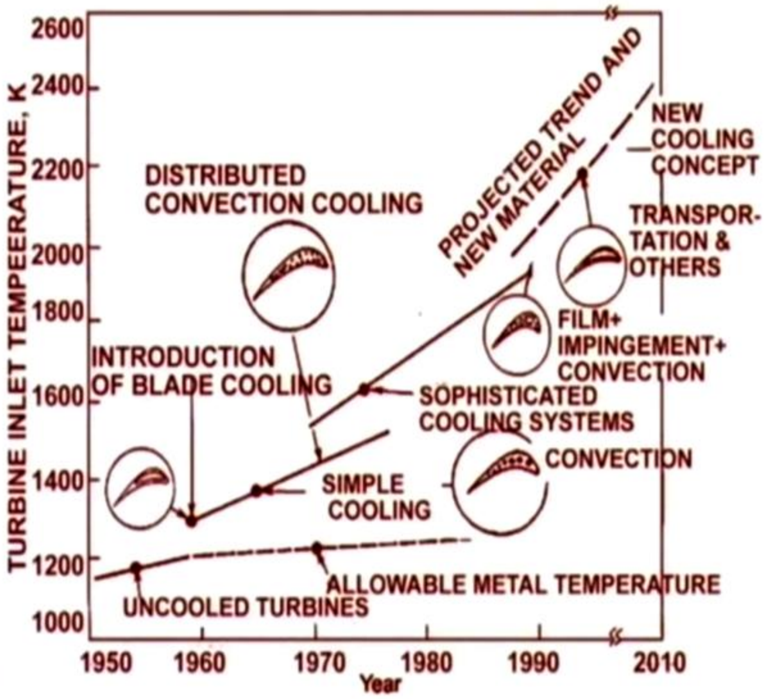

Figure1.1 Evolution of cooling system in gas turbine

It shows that initially in 1950 turbine blades are un-cooled which leads to low thermal efficiency therefore further improvement in cooling as simple cooling, distributed convection cooling, sophisticated cooling system and then Film impingement convection cooling system introduced and it also go for in new development of cooling system for improving heat transfer rate which leads to increase in thermal efficiency.

As we can see in figure1.2 that the jet impingement convection cooling system cools the turbine blades very efficiently and we can also see the amount of relative coolant flow is also reduced in it. In turbine power plant the blades which are at high temperature about more than 900º C require to cool its components very fast. It removes the heat very rapidly to cool the system and increase the thermal efficiency of Gas turbine Power plant. In high pressure turbine, blades have maximum temperature and maximum temperature gradient across both the router and the stator therefore plates are thermally loaded in cycles of operation sometimes turbine failure occurs mostly due to Creep i.e. thermal fatigue therefore instant impingement convection cooling system plays vital role in cooling, deter in thermal fatigue or to increase thermal efficiency.

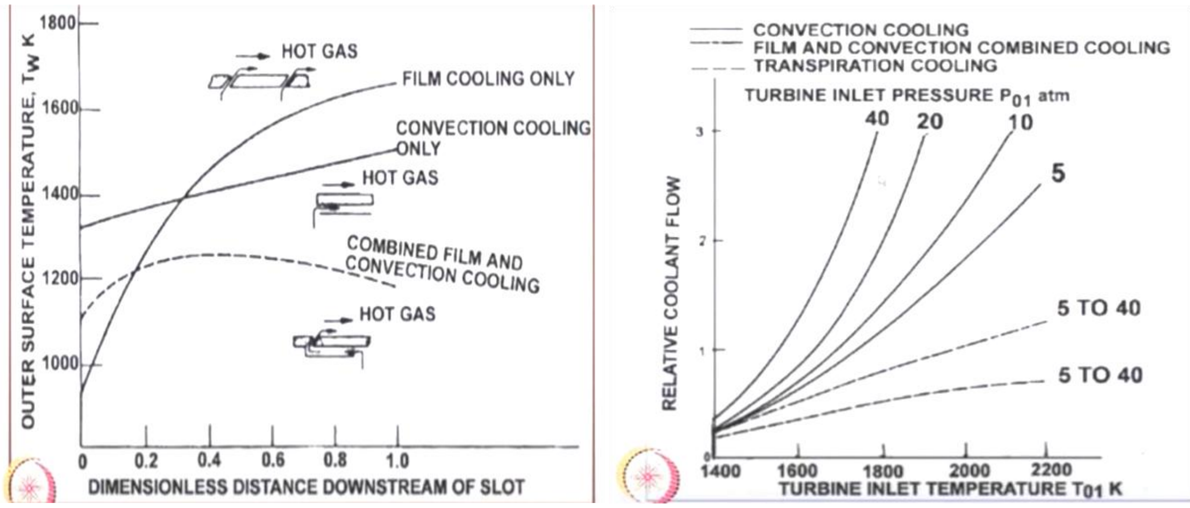

Figure1.2 Applicative diagram of gas turbine

The jet impingement cooling of the hot surfaces is also being used in nuclear power plants due to its capability of high heat removal rate. During the loss of coolant accident (LOCA) conditions in nuclear reactor, the cluster of clad tubes consisting of fuel rods becomes over heated even after the closure of reactor. Therefore, an emergency core cooling system (ECCS) is provided in the nuclear reactors to cool the clad tube under LOCA conditions. In an advance heavy water reactor, the water jet impingement cooling technique is used as a part of ECCS to cool the overheated clad tubes, under such conditions.

Due to the necessity of quenching process for industrial development, the scientists and researchers have carried many experimental and analytical studies for the sake of understanding quenching phenomena. Most of the researchers can be divided into two groups according to the main interest, the first group includes those who are interested in the mechanical properties of metals such as hardness, and the second group includes those who are interested in the mechanism of heat transfer during cooling process. In this study, a brief history about the literatures related to the second groups will be presented.

For liquid jet cooling on a hot plate, the assessment of the critical heat flux (CHF), which represents the largest cooling capacity for the jet cooling, is very important to understand the burnout phenomenon in nucleate boiling.

1.1. The objective of the research:

For liquid jet cooling on a hot plate, the assessment of the critical heat flux (CHF), which represents the largest cooling capacity for the jet cooling, is very important to understand the burnout phenomenon in nucleate boiling.

In order to understand the boiling heat characteristics of water jet more extensively, an experimental and numerical study was carried out to investigate jet boiling heat transfer characteristics of water jet impingement on a horizontally flat surface under the free surface jet condition. The main interest was focused on the effect of the jet velocity on the CHF points were systematically studied. The boiling heat transfer and the CHF for steel plate and aluminum were compared with each other. The purpose of the numerical and experimental study is to develop a good correlation between jet velocity and CHF points.

1.2. The scope of the research:

This project is tries to obtain an effect of jet velocity on CHF points; in other word we are tries to plot wall heat flux versus time and temperature versus time graph for different jet velocity for both plates. Also tries to determine in what proportion jet velocity effect CHF value. To achieve this goal, experimental setup was carry out all the heat transfer experiment and numerical modeling had been done to validate our experiment. The intial plate temperature and jet velocity are mainly involved in this research work. The flow visualization study was used to observe the jet impingement cooling process and provide some insights into the flow field of the jets.

CHAPTER 2

Literature Review:

This chapter reviews heat transfer concepts, numerical models, and experimental work relevant to the jet impingement. The discussion begins with an in depth review of previous research conducted on jet impingement cooling and the basic criteria used to evaluate their thermal performance. The main goal is to provide basic understanding of the mechanisms involved in jet impingement cooling and the effects of geometry, specifically for a sub-cooled, confined-circular water jet impinging on a flat heated surfaces. This discussion is followed by a review of previous research conducted on numerical modeling of two-phase flow, specifically the implementation of the k-ε turbulence, within the context of the Eulerian multiphase model, for wall boiling characterization.

Liu et al. (2002) have studied the film boiling heat transfer by Water jet impingement on a hot surface. They concluded that the primary mode of film boiling is strongly influenced by the degree of fluid's subcooling.
Mozumder et al(2007). conducted researches on quenching phenomenon via Water jet impingement on a sheet made of three different types i.e. steel, copper and brass with different velocities of Water jet from 3 to 15 m/s, subcooling temperature of 5-80 K and the initial sheet temperature of 250- 600 C. They concluded that the maximum heat flux increases with velocity of fluid jet and the fluid subcooling temperature.

Wolf et al. (1995) by conducting experimental works, concluded that convective heat transfer coefficient exceeds 10 kW/m K through a Water jet impingement to hot horizontal surface. Chan and Banerjee , in their study, indicated that quenching, as further continuous stability of liquid, is in contact with a hot surface, and quenching always appears when the temperature of the hot surface below the certain amount is related to Leiden frost temperature.
Iloeje et al. defined quenching as the beginning of transition boiling or a non-permanent boiling that is in transition from permanent film boiling to the nucleate boiling region, and expressed it in compliance with the minimum film-boiling heat flux on the boiling curve. Echi et al. experimentally conducted a research on transition of boiling heat transfer by Water jet impingement on a hot surface. In their study, they concluded that the heat flux at the stagnation point (central region) is more than other points in the radial region of the flow downstream, and by increasing the sub- cooling temperature of fluid and the velocity of fluid jet, the heat flux increases at the stagnation point.
Barnea and Elias(2013) conducted experimental and theoretical studies on flow and heat transfer areas during quenching of a heated vertical channel. They concluded that the leading edge is located in the transition boiling region and is developed between the dry and wet surface. Mitra et al. [8] investigated the boiling heat transfer aspect of water-TIO, and water-multiwalled carbon nanotubes (water- MWCNT) nanofluids based on laminar jet cooling of heated horizontal steel surface. They observed that in the present case, the shift from "film boiling to "transit ion boiling regime occurs earlier for nanofluid than that of water jet cooled surface.

Mitsutake and Monde(2006) in their experimental investigation on copper block reported a non-wetted stagnation region. The hot surface was hardly wetted within a short time immediately after the jet impingement, due to complete splashing of liquid jet in the form of small droplets.
Liu and Wang in their experimental investigation on stainless steel surface with 80°C sub-cooled fluid and initial surface temperature of 1000°C also suggested that within stagnation

region, transition boiling occurs instead of film boiling heat transfer. Since, the vapor layer thickness is only 3–5 mm, thus, fresh fluid touches the high temperature surface partially. The assumption of film boiling at the stagnation region is valid with the fluid of lower velocity and lower degree of sub-cooing.

Koldin and Platonov (2008)in their analytical investigation also assumed that heat transfer in the impingement zone proceeds initially from the mode of transition boiling and outside the impingement zone by the film boiling mode. With the flow of considerably lower temperature fluid over the hot surface, a thin and unstable layer of steam forms which does not create a considerable thermal resistance. The disturbance due to impact shock by the impinging fluid on the hot surface at the stagnation region prevents the formation of a stable steam film.

Ishigai et al. (1983) for a planer jet (Eq. I) and Ochi et al. for a circular water jet (Eq. II) proposed the following correlations to determine the minimum film boiling heat flux

$$q_{MFB} = 5.4 \times 10^4 (1 + 0.527 \Delta T_{sub})(U)^{0.607} \qquad \text{(I)}$$

$$q_{MFB} = 3.18 \times 10^5 (1 + 0.383 \Delta T_{sub}) \left(\frac{U}{d}\right)^{0.828} \qquad \text{(II)}$$

Karwa et al. (2011) in their analytical study has also proposed two separate correlations for minimum film boiling heat flux, q_{MFB}. These correlations are applicable for the stagnation region with a circular (Equation (7)) and a planer jet (Equation (8)).

$$q_{MFB} = 1.02 k_l \frac{\Delta T_{sub}}{d} (\mathrm{Re})^{\frac{1}{2}} (\mathrm{Pr})^{\frac{1}{2}} \qquad \text{(III)}$$

$$q_{MFB} = 0.70 k_l \frac{\Delta T_{sub}}{w} (\mathrm{Re})^{\frac{1}{2}} (\mathrm{Pr})^{\frac{1}{2}} \qquad \text{(IV)}$$

Narumanchi et al. (2008) developed a numerical model for boiling heat transfer in an impinging jet. The application of their study was in the cooling of power electronic components. They employed the Eulerian-Eulerian approach in Fluent software and found reasonable results for the prediction of wall superheat in the stagnation point region. However, no information was provided about the use of IAC and other interfacial force equations in their model.

Abhishek et al. (2013) numerically studied the effect of heater-nozzle ratio on the boiling phenomenon in an impinging jet. The jet Reynolds number was 2,500 with a subcooling of 20°C. They used the RPI model for decomposing the heat flux on the impingement plate and RNG k-ε to model the turbulence. The Eulerian-Eulerian two-phase flow model was used for the simulation. They found that irrespective of the heater-nozzle size ratio, at high superheat temperatures the quenching heat flux contributes to the major part of the heat flux. They also developed a correlation for the heat flux as a function of wall superheat and the size of the heater.

CHAPTER 3

Boiling Regimes during Transient Cooling

When a liquid jet flows along a hot surface whose temperature exceeds the rewetting temperature, the quench front advances in the direction of the flow. The quench front divides the heated surface into two zones: a quenched (wet) zone, a downstream, precursory cooling region (dry zone). And also during jet impingement cooling, the hot surface posses all the four mode of boiling simultaneously at different radial locations for a certain moment of time and distance. A typical surface cooling and boiling curve with coolant flow over the hot surface during the jet impingement quenching is shown in Figure 3.1. When a coolant jet strikes on to the hot surface, eventually a dark cooling zone is formed at the stagnation point. With time, this dark zone spread radially away from the stagnation point over the hot surface. The dark cooling zone comprises of two zones, that is, inner wet and outer boiling zone as marked by “AB” and “BC”, respectively, in the Figure 3.2.

The visible leading edge “C” of this cooling zone is termed as the wetting front. The dark

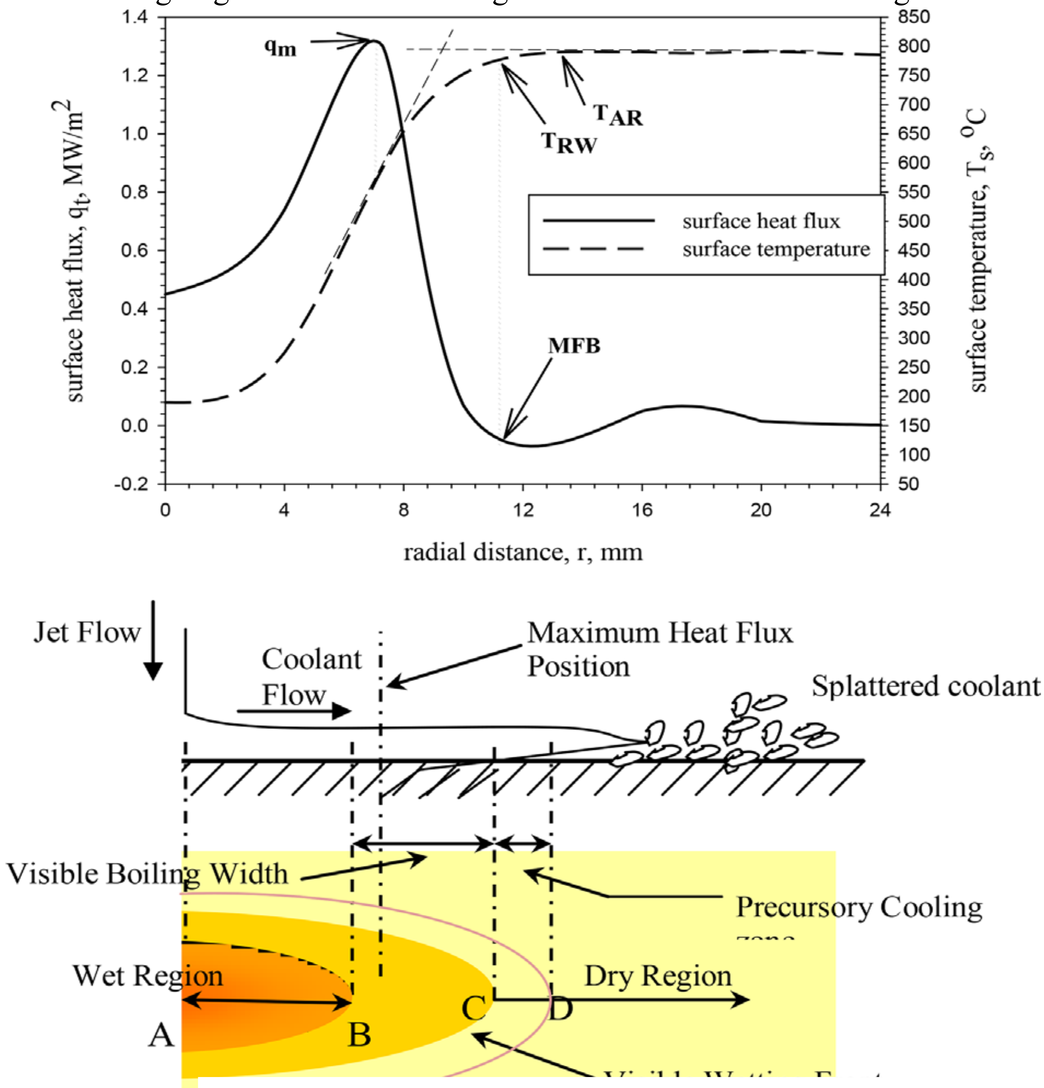

Figure3.1. Coolant flow and cooling curve.

inner wet zone “AB” is the most effective cooling zone of the hot surface. The temperature at the middle of wet zone is the least and is the regime of forced convection heat transfer, whereas, outer wet zone corresponds to the nucleate boiling regime.

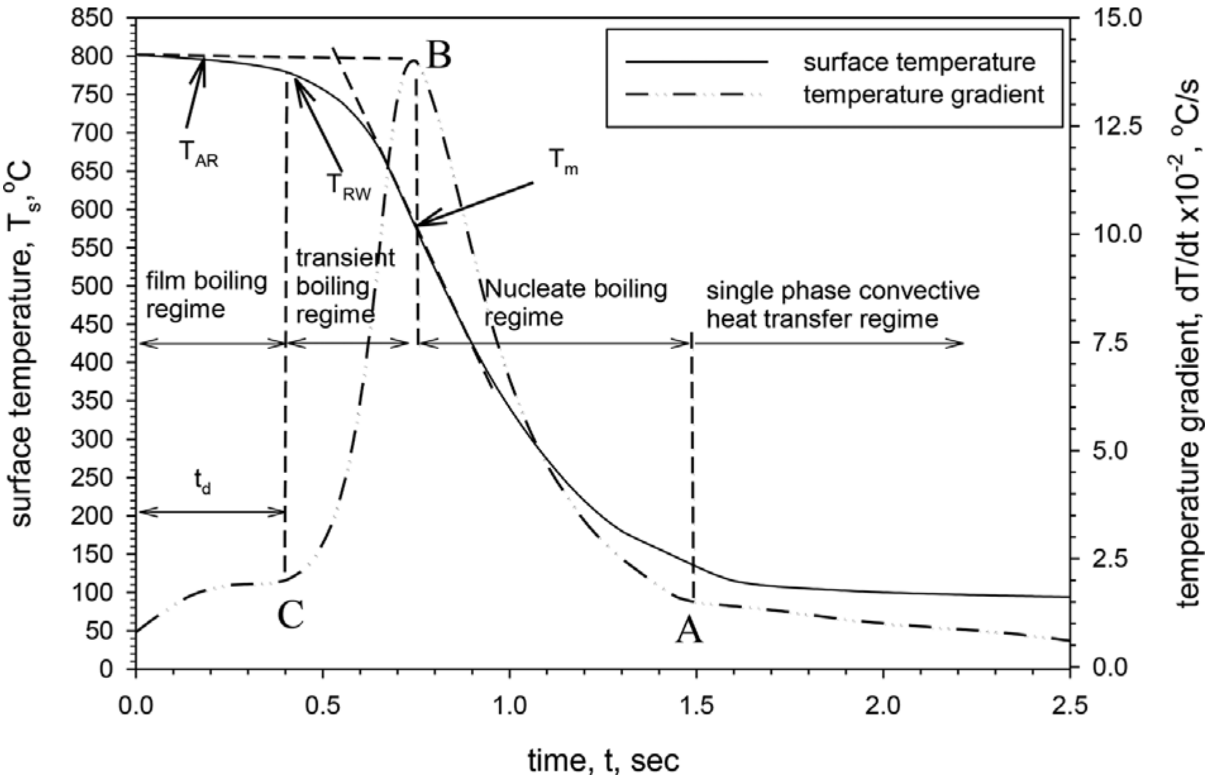

Figure 3.2. Surface cooling and boiling curve under transient cooling

The boiling zone, “BC” corresponds to the transition boiling regime, that shows the highest drop in surface temperature and the advent of maximum surface heat flux, q_m . The edge “C” where wetting front detach from the hot surface is the location of minimum film boiling point. The surface temperature at the minimum film boiling condition is considered as the rewetting temperature T_w. Immediate beyond the cooling zone, “AC”, the hot surface appears to dry but some amount of temperature gradient and the surface heat flux is observed for this region. This zone has been termed as “precursory cooling zone” marked as “CD” in the Figure 3.2.
The leading edge “D” of the “precursory cooling zone” is approximately the position where sharp drop in surface temperature is initiated or the point of apparent rewetting temperature. Though, the coolant has not yet covered this region but the heat is conducted through the solid surface from this precursory cooling zone to the comparatively inner cooling zone at the impingement point. Beyond precursory cooling zone the outer region is unaffected by the quenching phenomena, surface temperature is almost the same as the initial surface temperature before the commencement of jet impingement cooling. The heat transfer from this region is by convection, radiation (which is almost negligible) to the surrounding air and to a small extent by conduction to the supporting experimental apparatus. With the expense of cooling time, the relative position of these boiling regions shifts radially out ward away from the stagnation point, over the hot surface. When the complete hot surface is covered with the jet fluid, all the mode of boiling heat transfer vanishes. Finally at the end when steady state condition is reached, only single phase forced convective heat transfer take place from the entire hot surface within the wet region.

Similarly, any particular location on the hot surface exhibits these boiling modes, as cooling progresses. For a certain location on a hot surface, surface cooling and the temperature gradient curve with respect to time is shown in the Figure. All four different boiling regimes can be observed at any location on hot surface during jet impingement quenching that depends on surface initial temperature. Initially, film boiling regime is occurred over the hot surface, if the surface temperature is higher than the minimum temperature required for sustainable.

3.1. Film Boiling

It has been observed that there is consensus about the occurrence of film boiling regime for the entire locations on the cooling surface, except for the stagnation point. Soon after jet impinges on hot surface, the stagnation region undergoes through transient boiling to nucleate boiling before finally become wetted. However, out-side the wetted stagnation region, film boiling take place and shifts toward the downstream directions away from stagnation point with the elapse of cooling time. However, some researchers witnessed the momentary film boiling at the stagnation point as jet impinges on to the hot surface before the transient and other boiling regime. When a hot surface of the order of 900^{o}C and above is cooled with a stream of relatively cold fluid, the initial rate of heat transfer is limited due to occurrence of film boiling. As coolant impinges onto a high temperature surface, a thin layer of continuous vapor bubbles formed over the surface. This vapor layer prohibits the direct contact of liquid to the solid surface; hence, stable wetting of the hot surface does not possible. This vapor layer thickness increases rapidly at the edge of stagnation region due to reduction in pressure gradient. Earlier experiments have also reported the region of initial film boiling at the stagnation point with a liquid sheet over the test surface. The stable film boiling persists for a time ranging from less than a second to the several minutes, depending upon hot surface material, and other experimental parameters.

3.2.Transition Boiling

During quenching hot surface temperature reduces continuously due to supply of fresh sub-cooled fluid and leads to an intermittent solid-liquid contact. There is a lower temperature limit of the film boiling regime, called minimum film boiling temperature, TMFB, also referred as the rewetting temperature, TRW. Below this temperature transition boiling regime occurs over the hot surface and the cooling rate become higher than the film boiling regime Region BC. The transition boiling regime is considered as the combination of unstable film boiling and nucleate boiling, alternatively existing at a certain location on the hot surface. The transition boiling regime is characterized by a violent splashing of liquid sheet from the hot surface, which is formed over the hot surface during the initial film boiling. For the transition boiling regime the vapor generation is interrupted with high frequency solid liquid contacts and these vapors wiped out with coolant, in the flow direction over the hot surface. Timm et al. contrarily suggested that high degree of liquid sub-cooling and jet velocity, prevents the formation of vapor film for the transition boiling regime and the heat transfer is governed by the rapid growth and condensation of vapor bubbles. The condensation of vapor bubbles and the eddy diffusivity lead to a higher heat transfer and an intermittent solid-liquid contact. Hall et al reported that vapor blanket thickness is the highest at the minimum film boiling point. This vapor thickness reduces with the reduction in surface temperature to the condition where sustainable solid liquid contact occurs.

3.3.Nucleate Boiling

Nucleate boiling regime emerges from the point of maximum cooling rate, corresponds to the maximum surface heat flux, qm, also shown as point "B", in Figure. The maximum surface heat flux point is termed as critical heat flux, CHF in the pool boiling and the forced convective boiling experiments under steady state condition. The nucleate boiling regime comprises fully developed Nucleate Boiling regime and onset of Nucleate Boiling (ONB). The higher heat flux region of the nucleate boiling is referred as the fully developed nucleate boiling regime and lower range of heat transfer as onset of Nucleate Boiling. The Nucleate boiling regime is characterized by thin annular layer of violent boiling with homogenous and/or heterogeneous bubble nucleation. The coolant flows with some splashed liquid droplets at the outer periphery of nucleate boiling regime. Islam et al. reported momentary stagnate period for nucleate boiling regime that help in generating more bubbles at the leading edge. The vapor stream breaks the thin film of liquid, which was formed earlier in the transition boiling regime, into splashed droplets. At maximum surface heat flux point, vapor layer breaks out and establishes effective liquid surface contact or the fully wetted region, leads to rise in heat flux. The vapor bubbles in the wetted region are smaller in diameter and of short live, due to high shear rate within the liquid film. These bubbles slide along the hot surface before collapsing and may not able to reach at free surface of liquid layer over the hot surface. Therefore, the free surface of liquid in the wetted region appears smooth undisturbed and shiny. The thickness of the vapor layer above the hot surface is limited because of vapor condensation in the sub-cooled jet flow. At lower range of nucleate boiling, generation of discrete vapor bubbles ceases, surface temperature reduces and surface heat transfer takes place only due to local fluid motion. With the decrease in surface temperature and rapid progression of boiling front, the nucleate boiling shift to the single phase convective heat transfer regime. The surface temperature at which nucleate boiling regime occurs is slightly higher for jet impingement quenching, as compared to pool boiling and forced convection boiling. Moreover, the heat transfer rate or surface heat flux at a certain wall superheat is lower for jet quenching, as compared to the pool boiling due to complex hydrodynamics of liquid jet and the transient nature of heat transfer. Unlike other boiling regimes the parameters viz. jet velocity, fluid sub-cooling, jet diameter, jet impingement angle, hot surface orientation, and jet exit to surface spacing does not affect the nucleate boiling regime.

3.4. Maximum Surface Heat Flux(CHF)

During jet impingement surface quenching, the maximum surface heat flux position separates the transition boiling regime from the nucleate boiling regime (Point B, Figure 5). This maximum surface heat flux condition is referred as the critical heat flux (CHF) point, under the pool boiling and steady state jet impingement cooling condition Some researcher reported the position of maximum surface heat flux at the boundary of wetting front (Point C, Figure 4), whereas; some reported it a bit inside of the wetting front in the wetting zone.

CHAPTER 4

Water Jet Impingement theory

Water jets may normally be used to achieve enhanced coefficients for convective heat transfer by impinging on the hot steel surface. As shown in Figure 4.1, water jet is typically discharged into a quiescent ambient from a nozzle. Typically, the jet is turbulent and, at the nozzle exit, is characterized by a uniform velocity profile. With the surrounding air causes the free surface boundary of the water jet to be broadened potential core the velocity profile is non uniform over the entire water jet cross-section increasing distance from the exit, the momentum exchange between the water jet and the potential core, within which the velocity distribution is uniform to be contracted as the water flow continue away from the nozzle. Downstream of the potential core is non uniform over the entire water jet cross-section and maximum velocity decreases with increasing distance from the nozzle exit. The region of the flow over which conditions are unaffected by the impingement surface is termed the free jet.

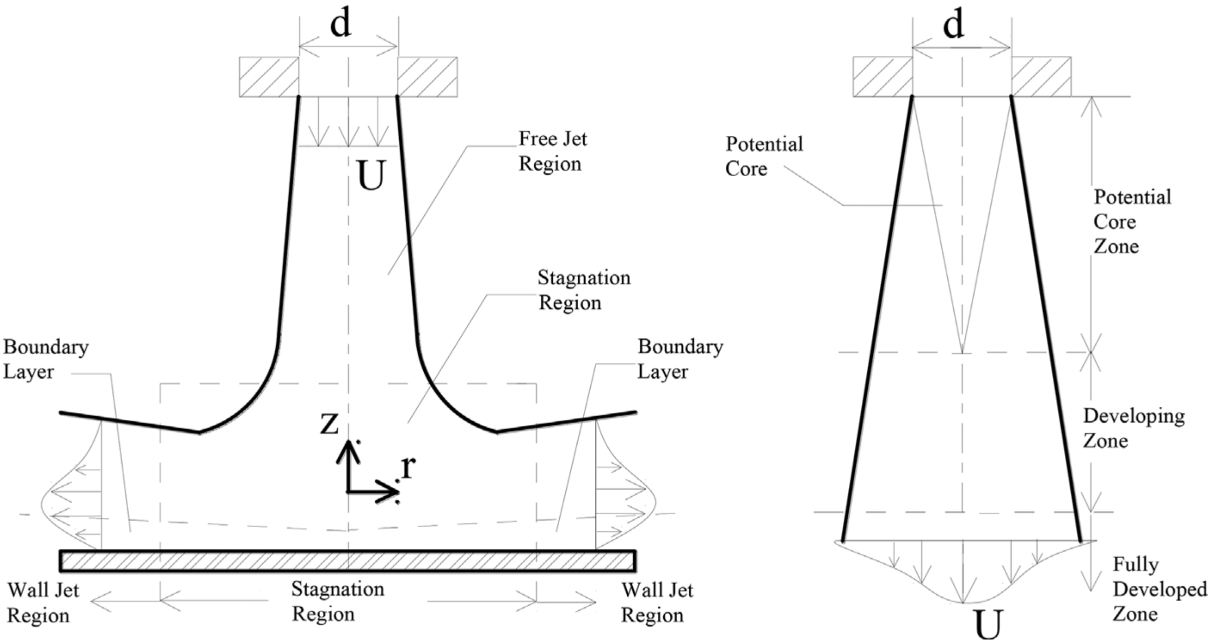

Figure 4.1.Schematic of impinging jet.

For water jet impingement cooling processes, there are a number of empirical models and theories relating to the way in which the steel section is cooled In general, there are two key assumptions, which relate to the accelerated cooling of steels:

1. There is no boiling present on the steel surface.

2. Stable film boiling is present on the steel surface.

Where, T_w and T_s is the water jet temperature at nozzle exit and initial plate temperature, accordingly, U or V_j is the jet velocity from nozzle exit and impinging on the target surface, accordingly.

In the case of no film boiling, it is assumed that the jet stream impact perpendicularly with the plate surface. Furthermore as the cooling water moves rapidly and forms turbulent conditions on the interface of water and plate, boiling conditions are suppressed

For the case of stable film boiling, it is assumed that a steady state condition develops at the water/plate interface. Essentially as the water is kept at a constant temperature and flow rate, a stable vapor layer forms on the steel surface. Since many theories supporting film boiling are dependent on experimental testing, hence they are restricted by any experimental assumptions.

As most water jet impingement models are based on experimentally derived data, it is necessary to observe all of the associated assumptions. Consequently to accurately analyze a water jet cooling process, it is necessary to conduct one's own experiments and develop an appropriate mathematical model

4.1. Jet Configuration

The cooling jet is broadly divided into three major group i.e. circular, planer, and spray (Figure 4.2),

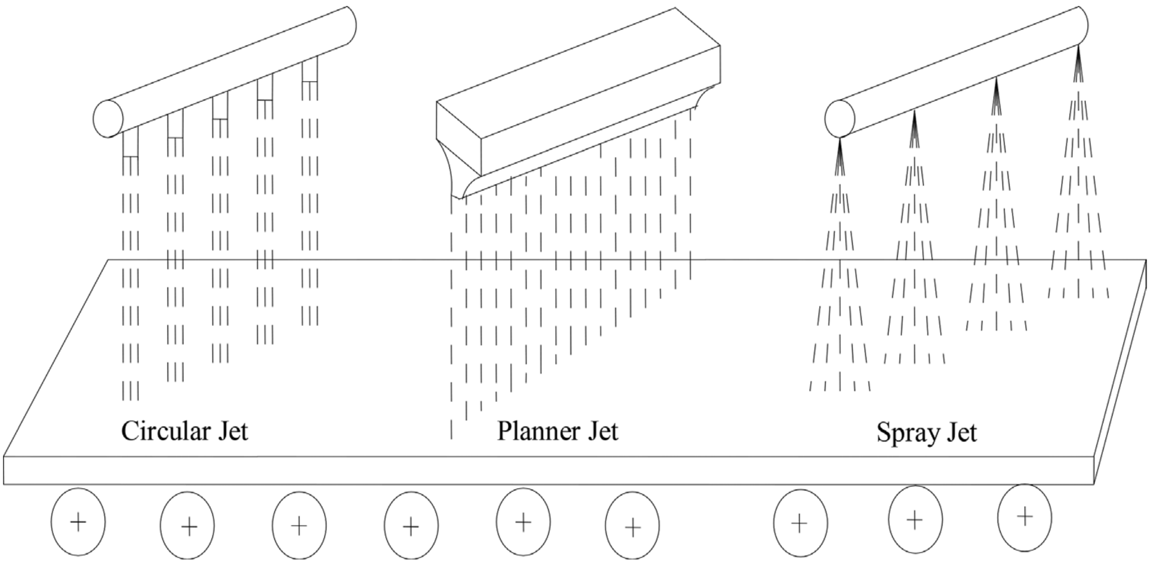

Figure 4.2. Categories of jet impingement cooling. (C. Agarwal et.al (2014))

Further, these may be as single jet or multiple jets array which depends on the rate of cooling desired. All these three types of jet have their own advantages and disadvantages.
The circular jet is normally preferred because of its effective penetration into the vapor film on the hot surface. In water curtain system, hot surface is cooled by a planer or slot jet, which spans entire width of the surface. One of the advantages of this jet is the uniformity of cooling in the surface’s transverse direction.

Jet impingement can further be configured as free surface jets, plunging jets, submerged jets, and confined jets (Figure 4.3).

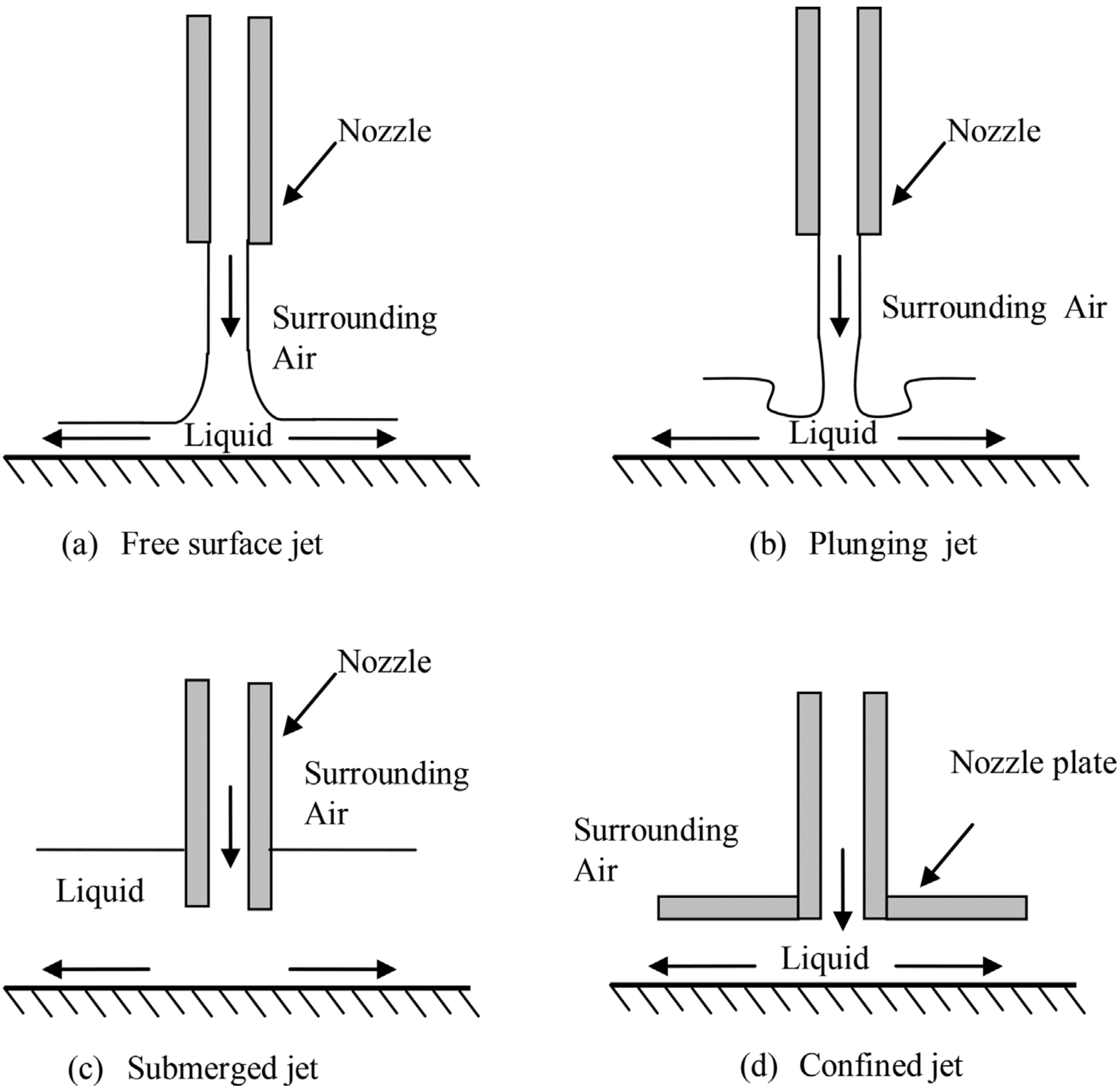

Figure 4.3 Jet configurations. (C. Agarwal (2019))

A free surface jet is the case where liquid jet exposed to a gaseous environment before impinging on an unconstrained flat surface. Unconstrained means, the coolant can flow off from the edges and does not pool on the surface. On a moving surface this can either be free surface or plunging jets depends upon the configuration. When the moving surface is cooled by array of water jets, the first row of jets are free surface jets but further downstream a layer of water is formed on top of the surface and the jets act as plunging jet. As the thickness of the water layer increases the effect of jet impingement decreases. Thus, for maximum heat transfer, all jets should be of free surface types.

Submerged jet conditions are those in which jet fluid is same as surrounding fluid, gas and air jet falls in this category. It has been reported that the heat transfer characteristics of submerged liquid jets are very much similar as gas or air jet impingement. However, heat transfer depends on Prandtl number of fluid, therefore, it should also be taken into account, while evaluating the quenching performance. The impinging jets can also be classified by their impinging direction, that is, whether the jet is oriented normally or obliquely with respect to the hot surface and on the basis of target surface, i.e. flat, convex, or concave. A jet is called sub cooled jet if the temperature of jet fluid is less than fluid saturation temperature

4.2. Rewetting Parameters

When the hot surface is quenched with the liquid jet, initially at stagnation point surface heat removal rate is limited due to formation of thin vapor film. After that the effective surface cooling takes place with the shift of film boiling regime to the unstable transient boiling regime. The partial solid–liquid contact establishes and with elapse of cooling time a stable wetting of hot surface occurs. The condition for initializing hot surface wetting is termed as the rewetting. Initially rewetting take place at the stagnation point, where, jet first strikes at the inception of the quenching process, thereafter, the rewetting condition progresses in the downstream direction, away from the stagnation point. As wetting of whole hot surface occurs, steady state condition reaches and singe phase heat transfer take place from the entire hot surface.

The rewetting phenomenon is evaluated on the basis of rewetting parameters viz. rewetting temperature, wetting delay, rewetting velocity, and the maximum surface heat flux. These rewetting parameters during quenching depend on various operating parameters pertaining to the hot surface and impinging fluid.

4.2.1. Wetting Delay

When, a liquid jet impinges on to the hot surface, the wetting front remains stagnant within the impinging region for a certain period, before its progresses over the hot surface. The time interval between application of the liquid jet and the initialization of wetting front spreading over the hot surface is termed as the wetting delay. Several researchers also described the wetting delay period as the resident time. Mozumder et al. and Hammad et al. observed that the radius of this small central region over which the wetting front remains stagnant during the resident time is invariable for a certain type of surface. As discussed earlier with the impingement of liquid jet on the hot surface, stable film boiling with un-wetted surface takes place at stagnation point. A liquid sheet over the blanket of vapor is formed, the size of sheet depends on the impinging fluid inertia and the surface tension force at the sheet edges. With time, two phase convective heat transfer and conductive heat transfer reduces the surface temperature for downstream locations and that initiate the progression of quench front away from the stagnation region. Akmal et al. on cylindrical surface of steel visualized similar phenomena of wetting front movement in three stages. The initial non-wetting stage, which, is followed by the spreading of wetting front and the final stage of a fully developed constant size wetted region. The non-wetting stage is found immediately after the jet impinges on the hot surface, which is characterized by the formation of a protective vapor layer on the hot surface with water splashing in the form of small droplets Mozumder et al. found the resident time or the wetting delay is a strong function of surface properties, surface initial temperature, coolant flow rate and degree of liquid sub-cooling. In addition Piggott et al. reported that the wetting delay also depends on heat generation rate and jet impact angle, while surface finish and surface size has negligible effect. Akmal et al. investigation has also indicated that wetting delay strongly depends on surface initial temperature and degree of liquid sub-cooling, however, marginally on the jet diameter. Agrawal et al. have reported that wetting delay does not depend on nozzle exit to surface spacing, z/d, and within stagnation region remains unaffected by jet diameter, jet flow rate, nozzle configuration, and surface orientation.

4.2.2. Rewetting Temperature

Basically the hot surface temperature at the rewetting condition is referred as the rewetting temperature there are two major groups of investigators, one who considered surface temperature corresponding to the minimum film boiling point or the onset of transition boiling regime, (TMFB), as the rewetting temperature. Another group who considered the surface temperature at the maximum surface heat flux condition as the rewetting temperature. The surface rewetting condition is followed by a sharp drop in surface temperature due to initialization of effective surface cooling and establishment of continuous solid-liquid contact. Therefore, some of the investigators have also considered the surface temperature as the rewetting temperature; at which sharp drop in surface temperature is observed on the temperature time plot. Some publications with film cooling also reported that the surface temperature corresponding to the maximum rate of change in temperature as the rewetting temperature. The rewetting temperature may be considered as the Leidenfrost temperature for the droplet and spray cooling system. The Leidenfrost temperature is generally defined as the maximum temperature at which an isolated droplet floating on a vapor cushion eventually collapses and touches the hot surface.

4.2.3. Rewetting Velocity

The rewetting velocity is the measure of hot surface wetting that take place during surface quenching, that is, how quickly a flowing fluid cools the hot surface. The time taken for wetting front to move or rewetting to occur between two marked locations on the hot surface is the unanimously adopted method of determining the rewetting velocity. However, Chan et al. has determined the rewetting velocity by taking the average of wetting front movement for three different regions, that is, for pre, post and within the quench front region.

The rewetting velocity increases with the increase in liquid sub-cooling, pressure, flow rate, jet velocity and the jet diameter, however, decreases with the rise in initial surface temperature and power input. The effect of jet flow rate on the rewetting velocity is more for the surface of lower initial temperature than the surface of higher initial temperature. The rewetting velocity for horizontal tubes are found nearly 20–30 percent lower than for the vertical tubes.

Mitsutake and Monde reported that on the hot copper surface wetting front movement is slower as compared to the steel surface, due to higher thermal inertia.

4.3. Effects of Jet parameters on quenching :

The characteristics of round impinging jets strongly depend upon several parameters such as Reynolds number, distance between the nozzle and the plate, nozzle geometry and the rate of turbulence introduced at the inlet to the domain (Manceau et al. 2014). Even many more parameters influence the characteristics of the jet impingement like hardness of the coolant.

Here we want to show how the hardness of the water could changes the wetting front velocity of jet impingements.
We took one coolant as RO water (TDS 40) and another was normal tap water (TDS 700).
Both having flow rate of 0.667 liter/minute and initial plate temperature = 450°C

Time	Hard water	RO water
t=0	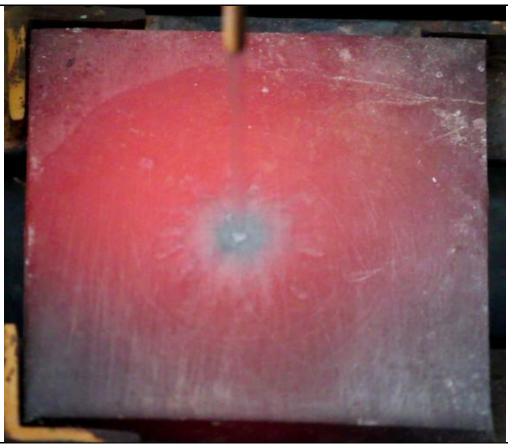	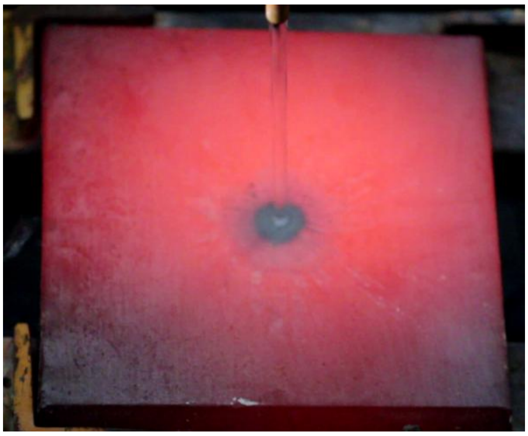
t=0.5s	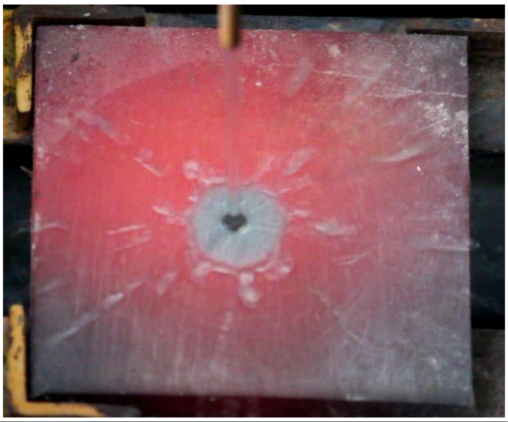	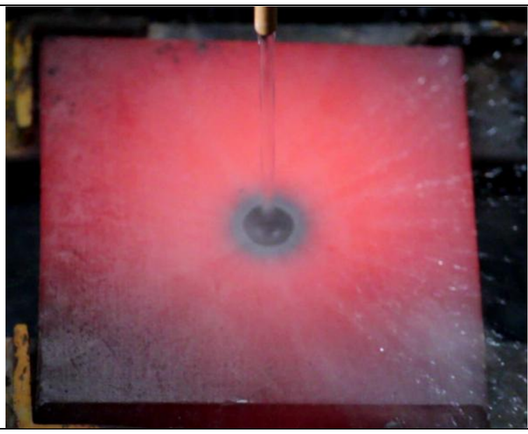

t= 1s	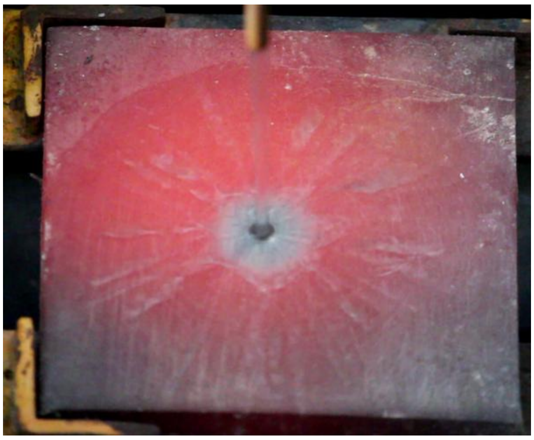	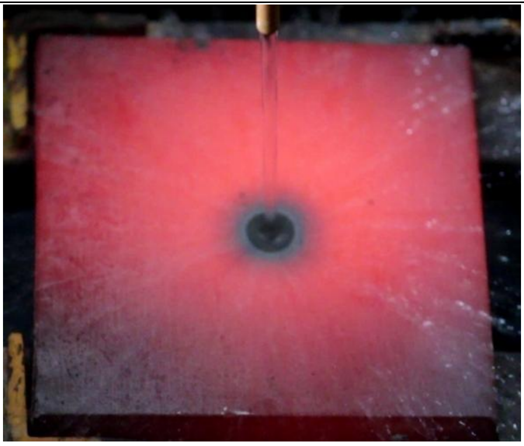
t=2s	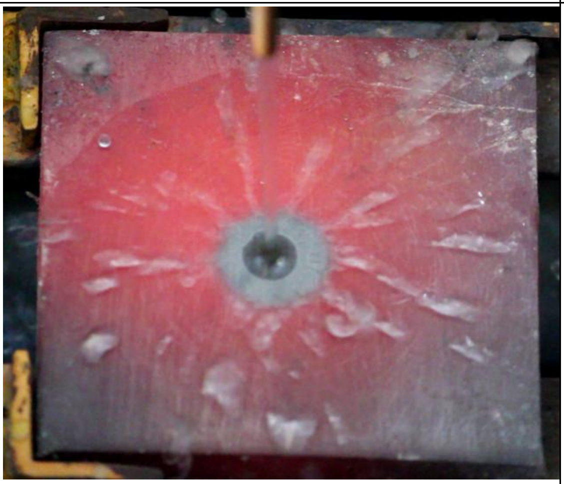	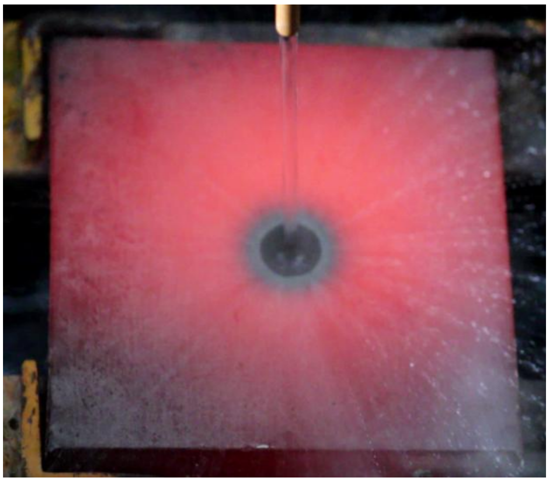
t=3s	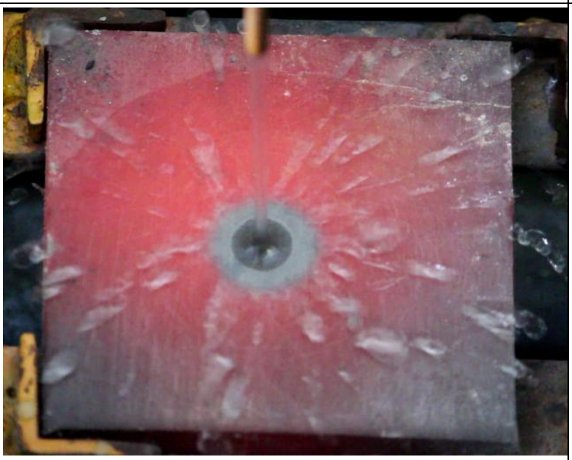	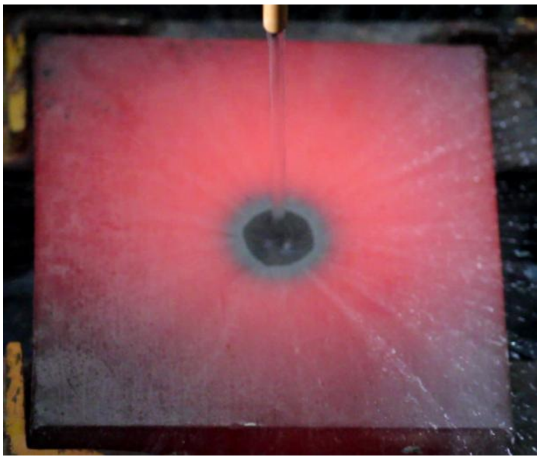

t= 4s	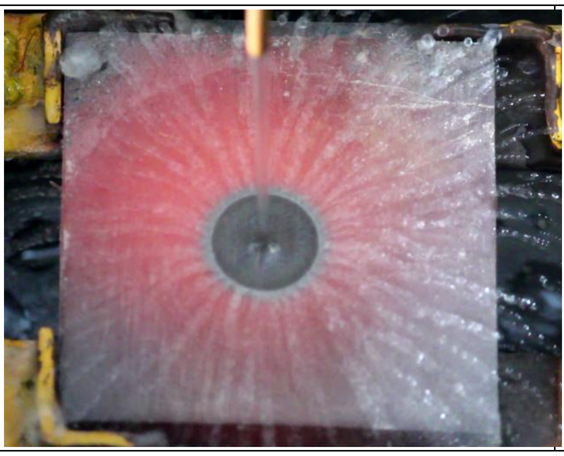	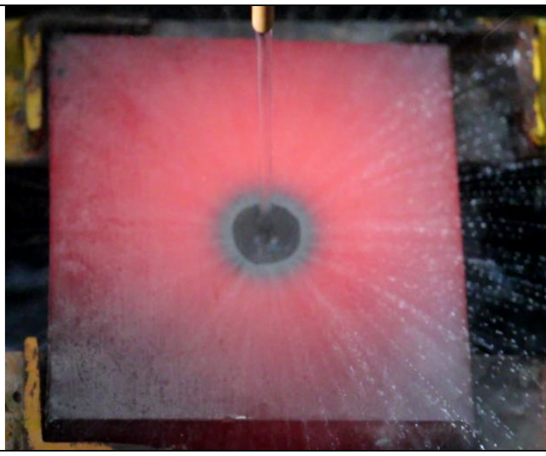

We can see from above images wet front velocity is more in hard water then RO water.

CHAPTER 5

Design and development of experimental set-up

First of all we decide the whole things which are setup design, nozzle size, SS series of Steel plates, open hearth furnace, Coolants we use are RO water, high TDS water.
After that we decided to a buy box from junk shop and then we clean it completely and overhaul any leakage or damage, unblock it with aerolite solutions or welding. Then we decided the paves inside the box for cart, leveling and outlet, etc.
After that we make a prototype of box and stand then worked in the welding and plumbing shop we made it and then colored the box black as shown in the picture (Figure5.1)

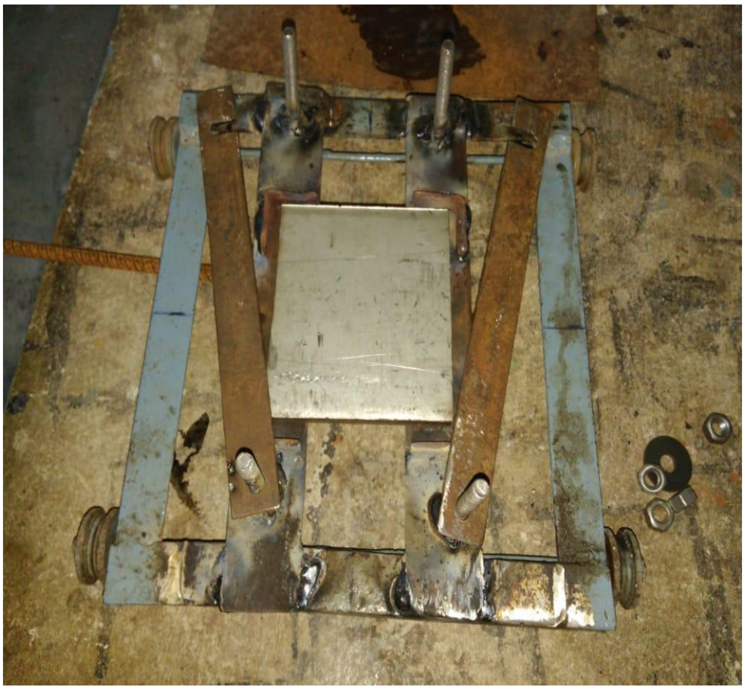

Figure5.1 Experimental Setup

For the paves for cart inside the box we attached two rods inside it in a slant position which remove liquid easily and at one corner of the box outlet is given to remove the liquid from box.

After that we make a design of cart which runs on the rods inside the box and carry the hot plate on which the jet is impinged.
According to the sketch we design the structure of cart as we attached 4 square angled to support the plate off size 100×100 mm and 10 mm of thickness on it. And two locks are also provided with the help of nut and bolt to hold the hot plate rigidly, we also provide four nudge on the structure of cart where plate is placed to reduce the contact between them which reduce intensity of loss of heat flux.

All these things are prepared by cutting and welding with the help of technicians in the welding and machine shops, as shown in the picture

At the last we adjust the level of all the components and structure with the help of leveler.

After that we bring the stainless steel plates of SS 310 of size 100×100 mm and check whether the size is fits on the cart stand, after that we noticed the dirt or slag on the surface of the steel plate then we decided to buff the surface of plates to clean it therefore we use the hand grinder and buffing tool which attached at the grinder side and buffed the all plates to clean the surface and to remove all dirt particles.

We also select the best surface and plates and give them priority to use in the experiment to get best desired result.

After fabricating all components of this base setup and pouring box and cart we stepped up to build the nozzle setup.

Figure 5.2 Isometric View of Setup

For the nozzle we decided to use copper capillary tube of refrigerator which have 3.14 mm in diameter and have length equal to 15 cm.[l/d > 4] it is a single jet straight height circular diametric nozzle which impinge the liquid jet onto the heated surface which z clapped on the cart setup inside the box.

As shown in the figure 5.2. of nozzle setup we attached the long nozzle with the reducer of copper with fullering the inside edge of copper nozzle and put appropriate amount of aerolite which further prevent any leakage.

After that to build the structure of pipes for flowing liquid , we decided to use U-PVC pipes , rubber tubes , nipple , bends , binding solution, etc to build structure. The reason is that U-PVC pipes is good in strength , rigidity and can withstand upto 50 to 60°C temperature .
First of all we sketch the structure on paper on which we gave two valves to have three different flow rates which are put in parallel.
In this structure as shown in images at one end nozzle is attached and on another end inlet rubber tube is attached this whole setup will attach on the main table and can be adjusted with the help of nuts and screws as per required heights. In this all the joints of pipes are jointed with the help of a permanent attaching solution to fix it rigidly and to prevent any leakage.
At the inlet side, inlet liquid is forced or pumped through a pump of 72watt.
The inlet liquid is stored in a tank which are placed at the bottom surface, and contain a pump to supply the liquid to nozzle.
During making this whole setup we failed 1-2 times to get the proper flow rates and appropriate results, but finally we build it.
Further the flow rates are adjusted using the control valves. The flow rate can be adjusted as follows

1) When we open both valves we get maximum flow, for water it is of around 1.3084 l/min
2) When we open former valve completely and later valve we get medium flow rate which is of about 0.1930 l/min
3) And when we close both valves we got minimum flow rate of 0.49476 L/min

Due to the lockdown in March we were not able to perform an experiment so we go for an alternate approach to achieve our goal. We were going with numerical analysis for our whole research work. We were getting our desired results by simulating our problem on ANSYS R1 2020 Fluent

So in the next chapter we are going to discuss some basic fundamentals of the Ansys Fluent review some literature work.

CHAPTER 6

Numerical Modelling:

Very few works on numerical simulation of the quenching through the liquid jet are reported in the literature, because of the complex mechanism, only empirical correlations developed to quantify the heat transfer rate. However, some of the researchers have contributed towards the enhancement of the understanding of the phenomena.

Hatta and Osakabe (1989) considers the laminar water curtains are impinging onto the steel plate for the numerical modelling. The laminar jet impinged onto the plate, and heat transfer led to the film boiling phenomena for quenching. It implies that the inertia force of the water jet in not enough to penetrate the vapour film formed near the heated surface. In industrial case, the water jet is always turbulent in nature as the jet Reynolds number is in the range of 30,000-50,000. Therefore, enough inertia of liquid can penetrate the vapour film, and film boiling cannot exist, and even at high wall superheat nucleate boiling can be established. Furthermore, nucleate boiling exhibited the more heat-flux than film boiling.

Hatta et al., (1989) did the numerical study on the quenching process of the heated steel plates by the water curtains. The numerical model gave quite satisfactory results with the measured value. However, they were unable to quantify the different boiling phenomena during the process in detail. Because of quenching phenomenon is very much Timm et al., (2003) proposed the mechanistic model for the jet impingement boiling phenomena. They assumed that due to the high wall superheat (> 800°C) large population of the vapor bubble generated near the surface and viscous sub layer could not exist. Furthermore, they took advantage of the Prandtl mixing length model to analyze the phenomena. Due to the growth, collapse, and the explosion of the bubbles created additional diffusivity in the flow. They emphasized on the fact that, one need more information about the bubble dynamics to improve the prediction of heat-flux. However, on the contrary, in the case of temperature controlled boiling the transition boiling phenomena, where heat flux decreases with increasing wall superheat, the mechanistic model by Timm et al., (2003) is unable to predict the heat flux. However, the concept of this model successfully implemented for the nucleate boiling by Omar et al., (2009).

Narumanchi et al. (2008) developed a numerical model for boiling heat transfer in an impinging jet. The application of their study was in the cooling of power electronic components. They employed the Eulerian-Eulerian approach in Fluent software and found reasonable results for the prediction of wall superheat in the stagnation point region. However, no information was provided about the use of IAC and other interfacial force equations in their model.

Abhishek et al. (2013) numerically studied the effect of heater-nozzle ratio on the boiling phenomenon in an impinging jet. The jet Reynolds number was 2,500 with a subcooling of 20°C. They used the RPI model for decomposing the heat flux on the impingement plate and RNG k-ε to model the turbulence. The Eulerian-Eulerian two-phase flow model was used for the simulation. They found that irrespective of the heater-nozzle size ratio, at high superheat temperatures the quenching heat flux contributes to the major part of the heat flux. They also

developed a correlation for the heat flux as a function of wall superheat and the size of the heater.
The numerical simulation of boiling heat transfer is performed by employing different two-phase flow methods. The Eulerian-Eulerian and Volume of Fluid (VOF) approaches are widely used for this purpose. The Eulerian-Eulerian method is more accurate because it solves the balance equations of mass, momentum and energy for both phases separately and they are more expensive than other models.

In this research work, the Eulerian technique is used to describe the flow. The basic concept of this approach is to observe the flow properties from a fixed location about a reference frame. The reference frame can be stationary or more generally moves at its own velocity. The Eulerian approach gives the values of the fluid variable at a given point (x, y, z) at a given time t. For example, the velocity can be expressed as V = V(x, y, z, t), where x, y, and z are independent of t.
Since the Eulerian approach is consistent with conventional experimental observation techniques, therefore adopted for mathematical formulations in the present work [Fagari and Zhang (2010)].

In order to mathematical formulations of the multiphase flow, there are three Euler- Euler approaches of multiphase models listed in the order of increasing accuracy:

- Homogeneous (Equilibrium) Model
- Multi-fluid Model
- Volume-of-Fluid (VOF) Free-Surface Model

In the multi-fluid model, all conservation equations are solved for each phase. From the numerical perspective, the Volume-of-fluid (VOF) model is very similar to the homogeneous model. A single momentum equation is computed for all phases that interact using the VOF model. However, the calculation of volume fraction equations using VOF model is considerably more accurate allowing the sharp resolution of the interfaces. One of the common defects of the VOF calculation can occur when the interface is not resolved sharply despite the use of the high-order discretization techniques for the volume fraction equation – in that case, the VOF model degenerates into the homogeneous model. This is quite common in many practical calculations. It happens due to very high-resolution requirements of the VOF model that can often be hard to fulfil.

6.1. Geometry

In Ansys Workbench R1 2020 Academic Version, using Fluent Module, we draw our physical model with help of either by Design Modular or Space-claim. We are going with design modular because in our problem we have contact region between plate and fluid domain so it will easy to draw in design modular using Boolean operation.

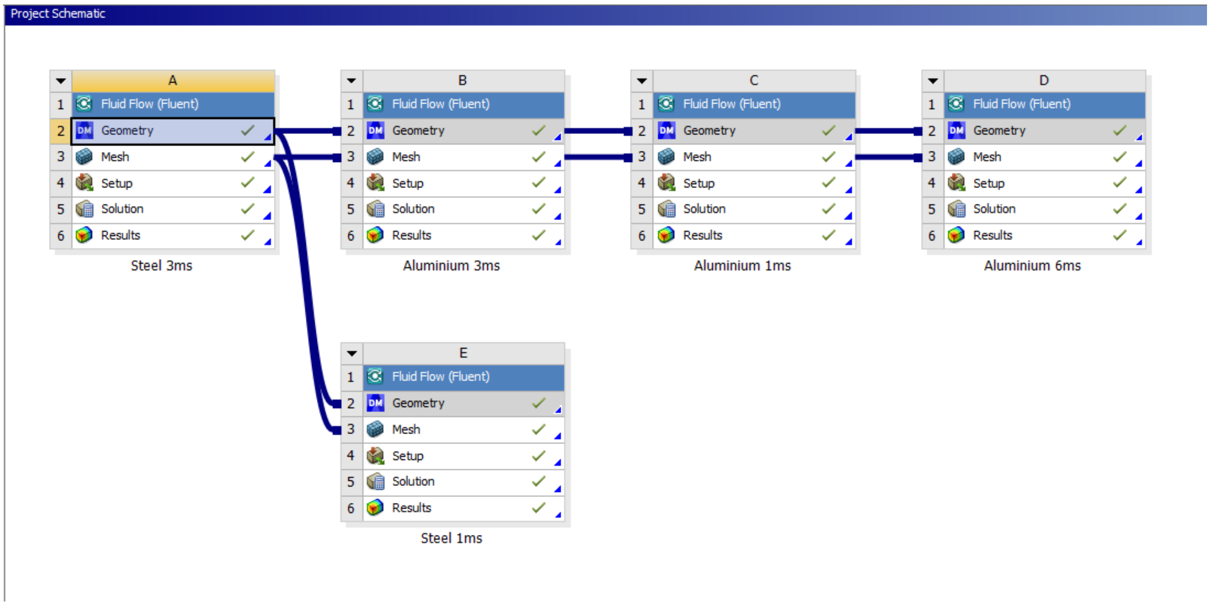

Figure 6.1 Window of ANSYS

Boolean operations consists: Add, Subtract, Unite, Body Delete, Part etc

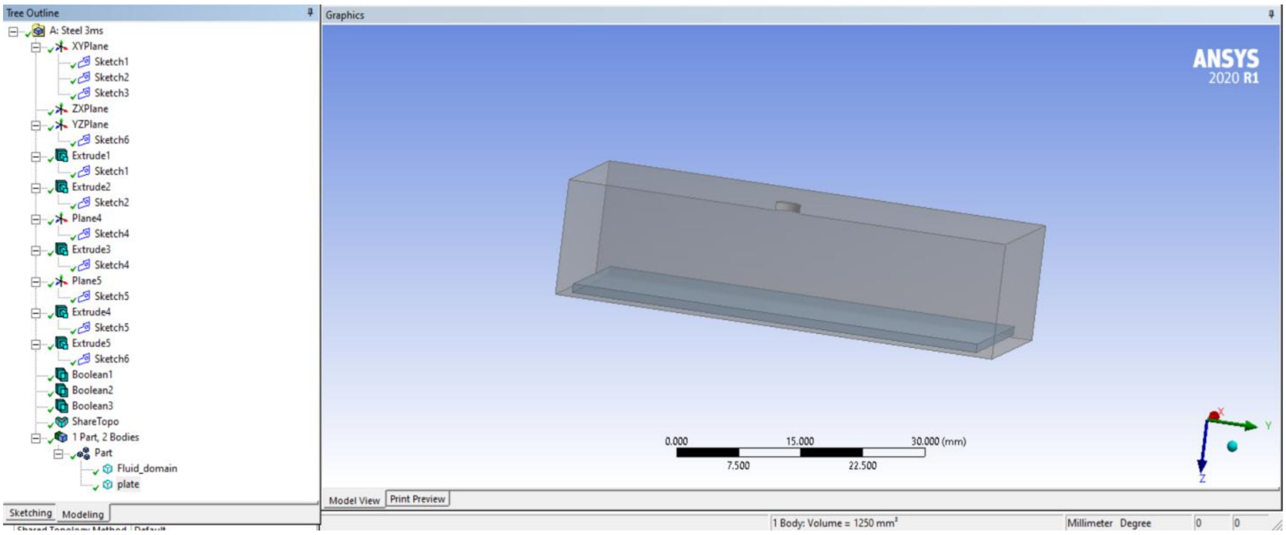

Figure 6.1. Geometry in ANSYS

Since our objective is to determine heat characteristics of jet impingement on plate.

Here we take the following parameters

Nozzle diameter = 3mm

Nozzle plate distance= 12 mm (fixed)

Plate material: Steel and Aluminium

Plate dimensions: 50 x 50 mm^2 x 1 mm (thickness)

Inlet Velocity: 1m/s, 3m/s.

Brief Images of Steps which are used to make our project problem:

Sketch- Extrude-Boolean operations-Unite-Subtract-delete body-Subtract

As you above images you will find that we take only half section of total computational domain. Because due to axis symmetry in our problem we can reduce our computation cost by considering only half part of problem. This also leads to reduce the total number of element in the Meshing.

After completing the geometry going for meshing

6.2. Meshing

By the definition, **Meshing** is an integral part of the simulation process where complex geometries are divided into simple elements that can be used as discrete local approximations of the larger domain. The **mesh** influences the accuracy, convergence and speed of the simulation.

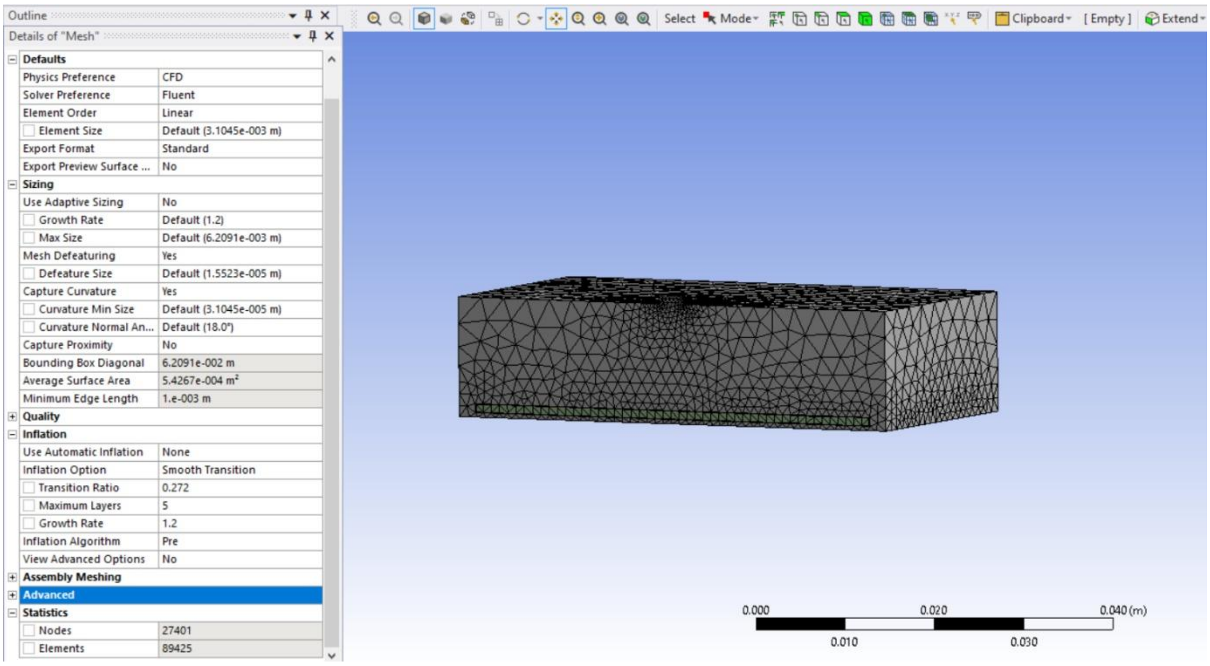

Figure 6.3. Meshing

It implies that finer meshing we will give more accurate results; this also leads to increase in computational cost.

In Academic version, there is restriction on number of mesh elements i.e. 512000 cells element so we can’t mesh our problem more than 512000 elements.

After generate meshing.

ANSYS FLUENT will try to move interior nodes to improve the **skewness** of cells with **skewness** greater than this value. By default, Minimum **Skewness** is set to 0.4 for 2D and 0.8 for 3D. We have skewness of 0.9

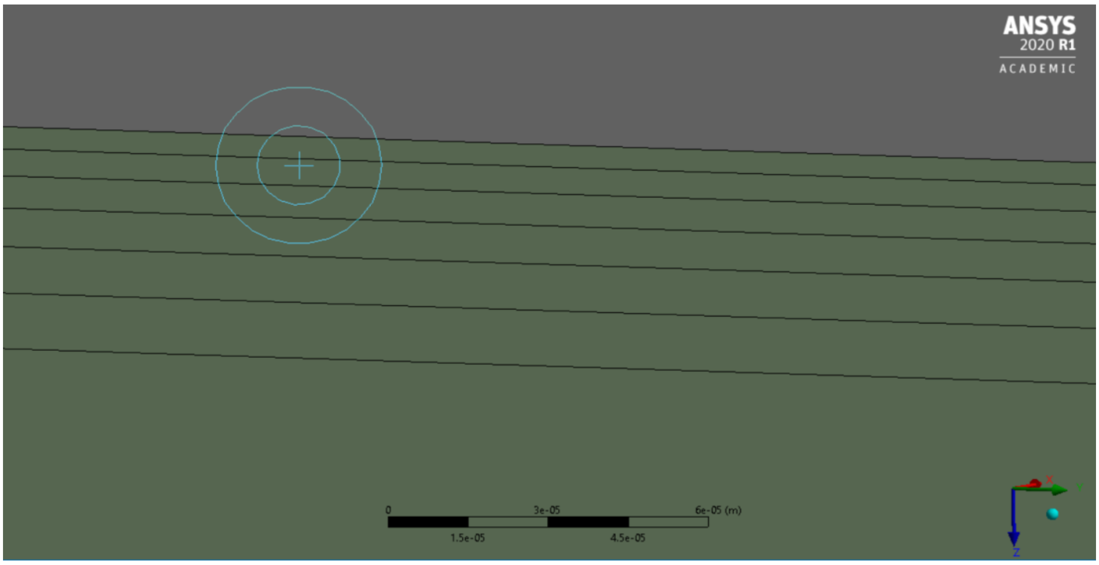

Figure 6.4 Inflation Layers

We provide inflation layer to the plate boundary in meshing

There are two reasons behind it.

The slope dT/dy will maximum at the wall and minimum at the thermal boundary layer so because it changes very fast in the lower regions or near the wall Therefore we need very fine mesh over here (lower regions). This will be done by inflation layer i.e. finer mesh near the wall and become coarser up above. Since we are not using small elements or we can say more element and using lot of elements were we need it so that is why we need inflation layers, see figure 6.4.

Provide name selection to each and every entity in the model.

Name selection for our model given below:

Inlet (jet inlet)

Outlet (opposite face of the cube)

Symmetry

Plate

Fluid_ domain

Remaining are named as Wall

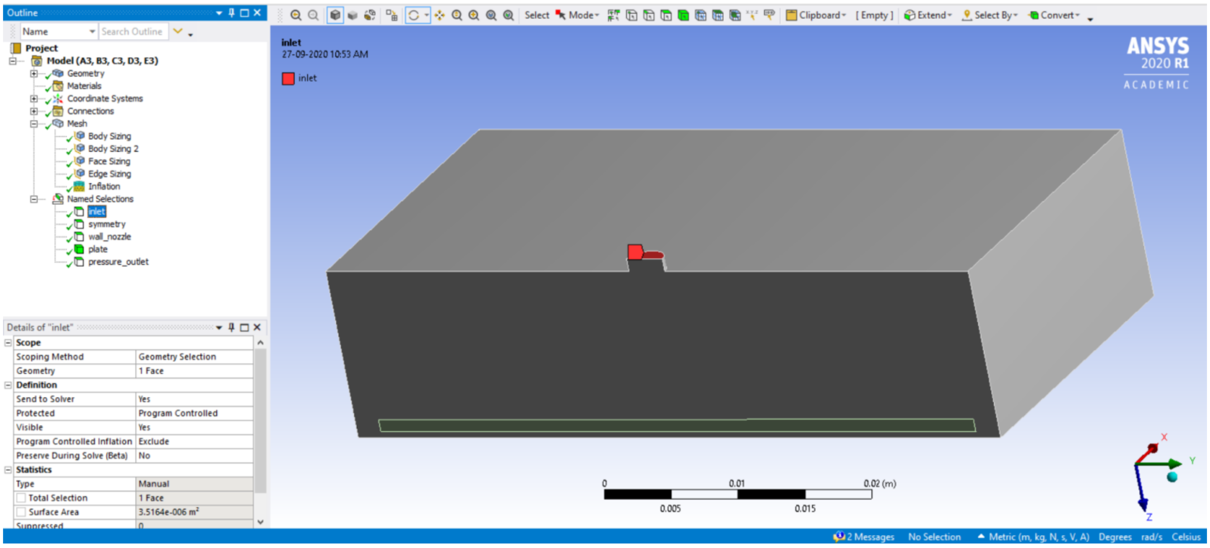

Figure 6.5 Name Selection List

Name selection is very important step in meshing because they will use in set up condition in the future.

Now update the meshing and close the mesh module

Click on setup.

6.3. Setup Conditions.

After review the literature, Eulerian- Eulerian multiphase VOF model is suitable for simulating the quenching of the plate using jet impingment.

In CFD, the volume of fluid (VOF) method is a free-surface modeling technique, i.e. a numerical technique for tracking and locating the free surface (or fluid-fluid interface). It belongs to the class of Eulerian methods, which are characterized by a mesh that is either stationary or moving in a certain prescribed manner to accommodate the evolving shape of the interface. As such, VOF is an advection scheme—a numerical recipe that allows the programmer to track the shape and position of the interface. The VOF formulation relies on the fact that two or more fluids (or phases) are not interpenetrating. For each additional phase that you add to your model, one variable is introduced: the volume fraction of the phase in the computational cell. In each control volume, the volume fractions of all phases sum to unity. The fields for all variables and properties are shared by the phases and represent volume-averaged values as long as the volume fraction of each of the phases is known at each location.

Thus the variables and properties in any given cell are either purely representative of one of the phases, or representative of a mixture of the phases, depending upon the volume fraction values.

6.3.1. Mathematical formulation :

Governing equations:

The turbulent three dimensional Navier-Stokes and energy equations are solved numerically by a finite volume scheme to simulate the thermal and turbulent and laminar flow fields.

The following assumptions are used:

(1) Three-dimensional turbulent flow
(2) Unsteady flow
(3) Incompressible fluid
(4) Constant fluid properties
(5) Negligible radiative heat transfer

Tracking the interface between the phases have been carried out by solving the continuity equation for the volume fraction of one (or more) of the phases. For q_{th} phase, the equation is as follows:

$$\frac{1}{\rho_q}\left[\frac{\partial}{\partial t}\left(\alpha_q \rho_q\right) + \vec{\nabla}.\left(\alpha_q \rho_q \nu_q\right) = S_{\alpha q} + \sum_{p=1}^{n}\left(\dot{m}_{pq} - \dot{m}_{qp}\right)\right] \qquad (1)$$

Continuity Equation of the fied:

$$\vec{\nabla}.\left(\rho\vec{v}\right) = 0$$

Energy equation of the field

$$\frac{\partial}{\partial t}(\rho E) + \vec{\nabla}.\left(\vec{v}(\rho E + P)\right) = \vec{\nabla}.\left((k_f)\vec{\nabla}T\right)$$

where,

$$E = \frac{\sum_{q=1}^{n}\alpha_q \rho_q E_q}{\sum_{q=1}^{n}\alpha_q \rho_q}$$

We use k-ε model after review the literature. The standard k-ε model based on the model transport equations for the turbulence kinetic energy k and its dissipation rate ε. The transport equation for k is derived from the exact equation, whereas ε is obtained from physical reasoning and has little resemblance to its mathematically exact counterpart. The transport equation for k and ε are given as follows:

(1) *Transport equation for k*

$$\rho\bar{u}_j\frac{\partial k}{\partial x_i} = \frac{\partial}{\partial x_j}\left[\left(\mu_l + \frac{\mu_t}{\sigma_k}\right)\frac{\partial k}{\partial x_j}\right] + \mu_t\left(\frac{\partial \bar{u}_i}{\partial x_j} + \frac{\partial \bar{u}_j}{\partial x_i}\right)\frac{\partial \bar{u}_i}{\partial x_j} - \rho\varepsilon \qquad (2)$$

(2) *Transport equation for ε*

$$\bar{u}_j\frac{\partial \varepsilon}{\partial x_i} = \frac{\partial}{\partial x_j}\left[\left(\mu_l + \frac{\mu_t}{\sigma_\varepsilon}\right)\frac{\partial \varepsilon}{\partial x_j}\right] + C_1\mu_t\frac{\varepsilon}{k}\left(\frac{\partial \bar{u}_i}{\partial x_j} + \frac{\partial \bar{u}_j}{\partial x_i}\right)\frac{\partial \bar{u}_i}{\partial x_j} - C_2\rho\frac{\varepsilon^2}{k} \qquad (3)$$

where

$$\mu_t = C_\mu \rho\frac{k^2}{\varepsilon} \text{ and } \mu_{eff} = \mu_l + \mu_t$$

The closure coefficients that appear in the above equations are given by the following values:

$$C_\mu = 0.09, \quad C_1 = 1.44, \quad C_2 = 1.92, \quad \sigma_k = 1, \quad \sigma_\varepsilon = 1.3$$

The governing differential transport equations were converted to algebraic equations before being solved numerically. The finite volume scheme which involves integrating the governing equations about each control volume yielding discrete equations that conserve each quantity on a control volume basis was applied to Eqs. (1) (3).The first-order upwind discretization method is applied to the convective fluxes in the momentum, energy and turbulence equations. The coupling between pressure and velocity was achieved by the SIMPLE algorithm. The convergence criterion for the conservation of mass, momentum and energy equations are considered 10 5, 10 and 10, respectively. At Re < 1000 the flow field exhibits laminar flow properties. At Re > 3000, the flow has fully turbulent features. The implicit method is used for time discretization.

6.3.2. Boundary Conditions:

As shown in Fig. 1, the nozzle inlet is on the top of the system, and the working fluid is water. The conditions of a subcooled Water jet impingement on a hot flat plate are considered at the temperature of 450 °C, with dimensions of 50 x 50 mm, and the thickness of the plate is 1 mm. Nozzle diameter is 3 mm and is located at a height of 12 mm from the top of hot surface. In the present study, approximately 89425 cells have been used. This grid is sufficient to ensure that all steep gradients in the flow and temperature fields are well resolved. The time step is equal to 0.1 s.

In this study, in the first simulation, velocity of fluid jet for ΔT_{sub}=27 °C has been changed from 1 m/s to 3 m/s. In addition, in the second simulation, we use same parameters for aluminum.

Properties of steel and aluminium are show in figure taking from ansys fluent data base

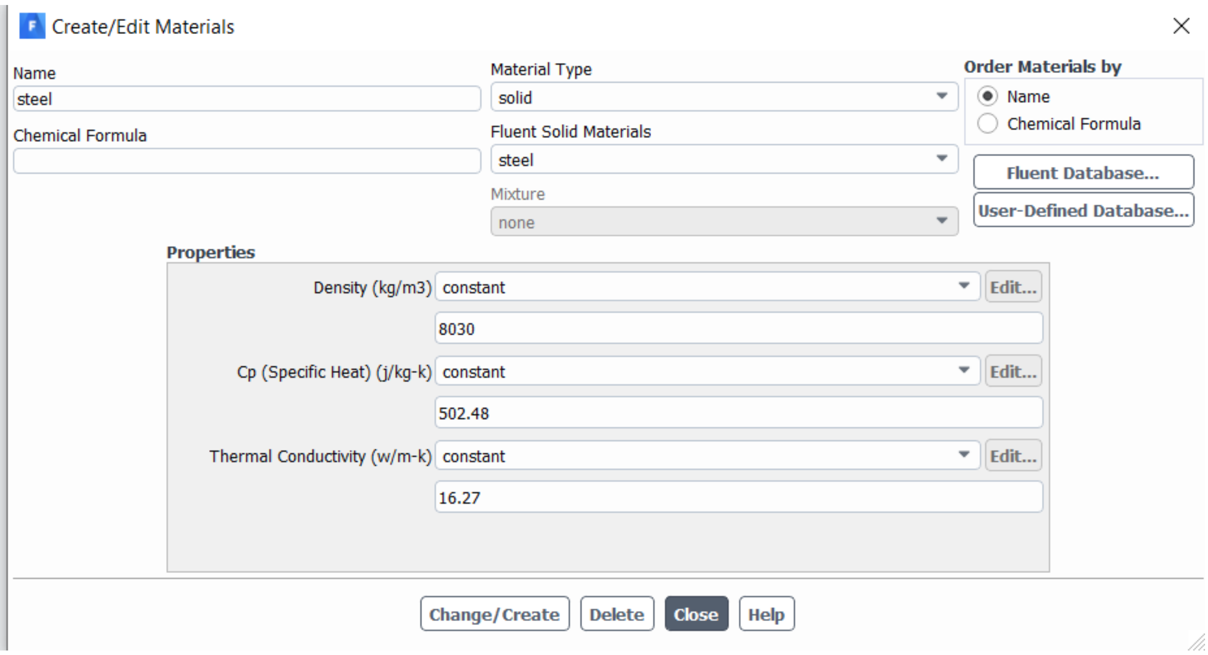

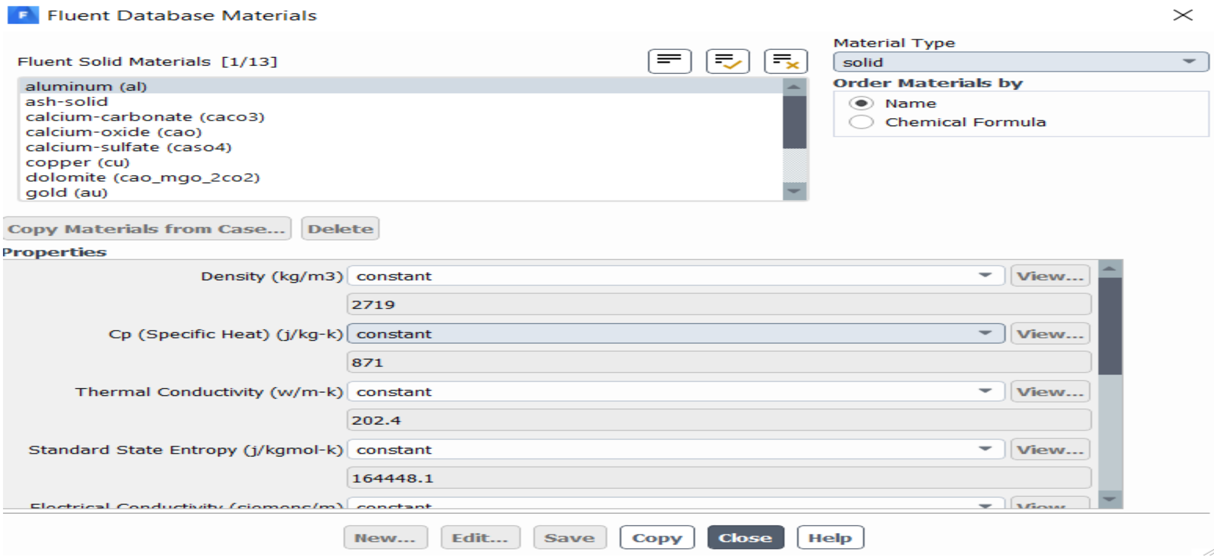
Fluent Database Materials
Fluent Solid Materials [1/13]
aluminum (al)
ash-solid
calcium-carbonate (caco3)
calcium-oxide (cao)
calcium-sulfate (caso4)
copper (cu)
dolomite (cao_mgo_2co2)
gold (au)
Material Type
solid
Order Materials by
Name
Chemical Formula
Copy Materials from Case...
Delete
Properties
Density (kg/m3)
constant
View...
2719
Cp (Specific Heat) (j/kg-k)
871
Thermal Conductivity (w/m-k)
202.4
Standard State Entropy (j/kgmol-k)
164448.1
New...
Edit...
Save
Copy
Close
Help

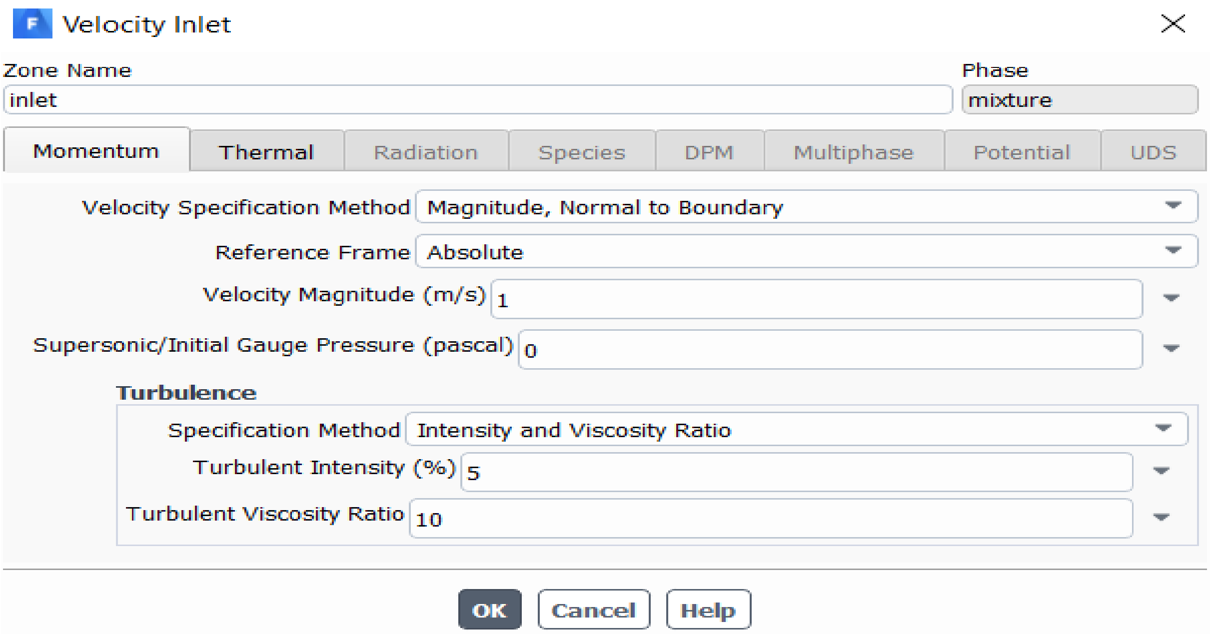
Velocity Inlet
Zone Name
inlet
Phase
mixture
Momentum
Thermal
Radiation
Species
DPM
Multiphase
Potential
UDS
Velocity Specification Method
Magnitude, Normal to Boundary
Reference Frame
Absolute
Velocity Magnitude (m/s)
1
Supersonic/Initial Gauge Pressure (pascal)
0
Turbulence
Specification Method
Intensity and Viscosity Ratio
Turbulent Intensity (%)
5
Turbulent Viscosity Ratio
10
OK
Cancel
Help

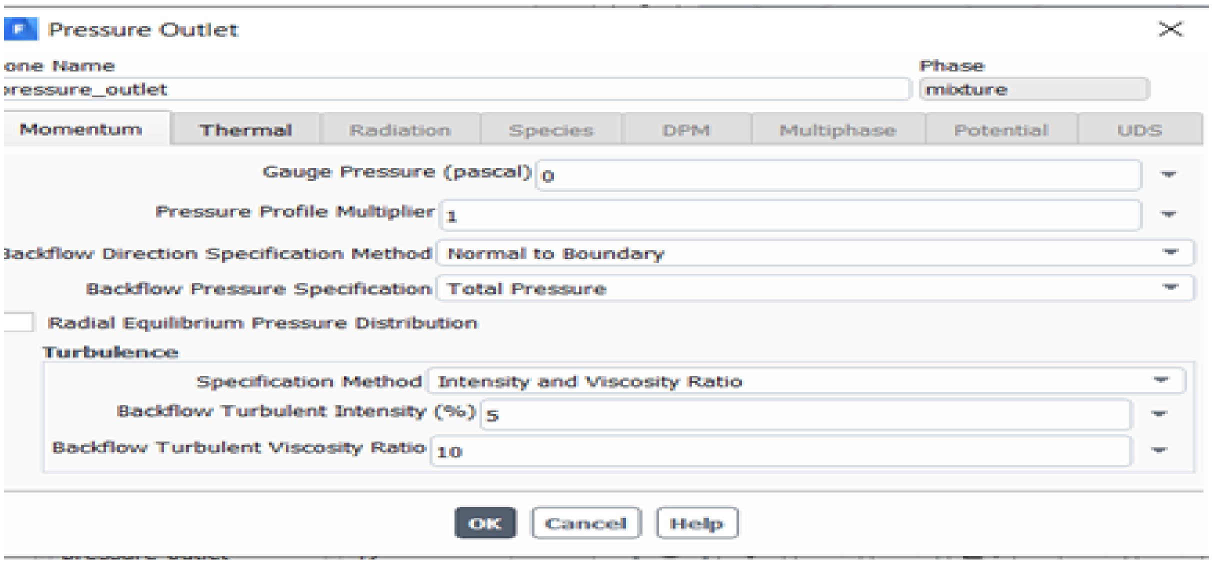
Pressure Outlet
Phase
mixture
Momentum
Thermal
Radiation
Species
DPM
Multiphase
Potential
UDS
Gauge Pressure (pascal)
0
Pressure Profile Multiplier
1
Normal to Boundary
Backflow Pressure Specification
Total Pressure
Radial Equilibrium Pressure Distribution
Turbulence
Specification Method
Intensity and Viscosity Ratio
Backflow Turbulent Intensity (%)
5
Backflow Turbulent Viscosity Ratio
10
OK
Cancel
Help

CHAPTER 7

Results and Discussion

In this chapter, the results are obtained from CFD Post analysis is presented. We can obtain various results. We are going to present only Wall Heat flux, Temperature plot. Wall heat transfer coefficient at different spatial location i.e. at stagnation point, 5mm 10mm, 15mm, 20mm distance from stagnation point for steel and aluminium plate

7.1. Steel Plate:

Wall Heat Flux Plots for V_j= 1m/s and 3m/s

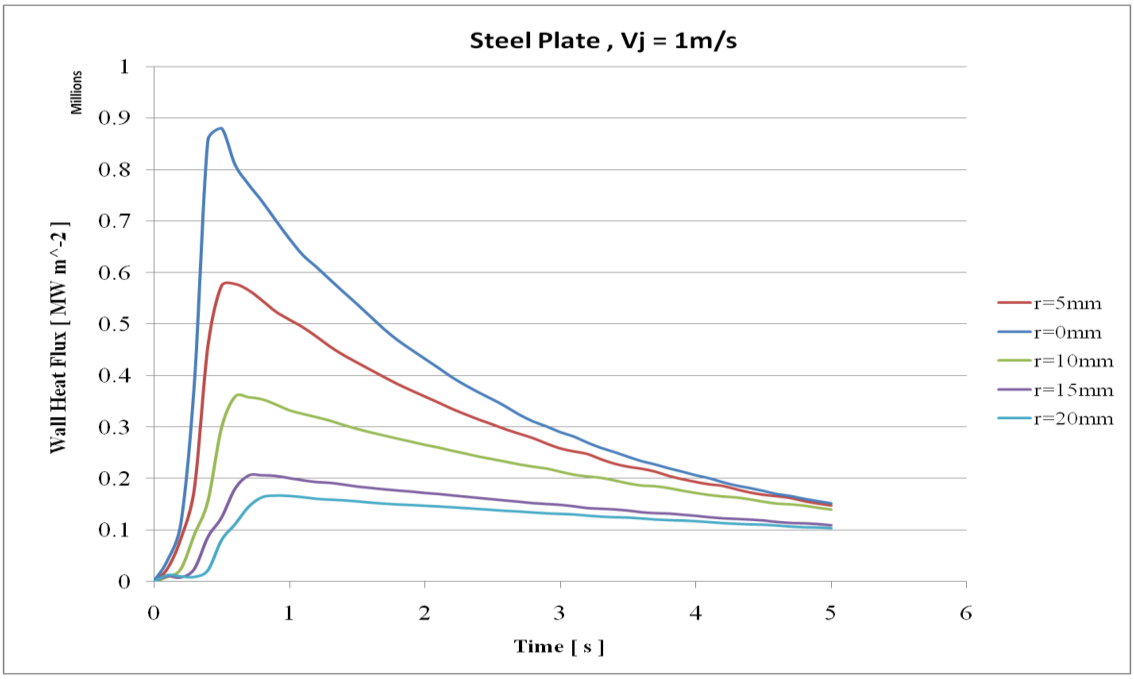

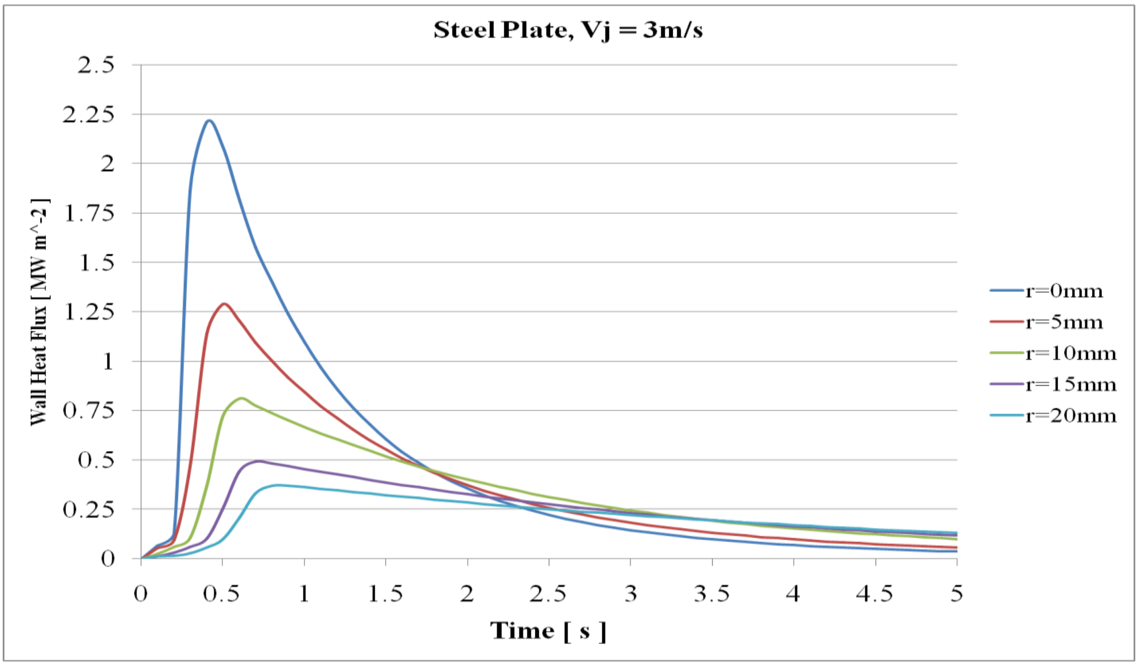

Temperature plots

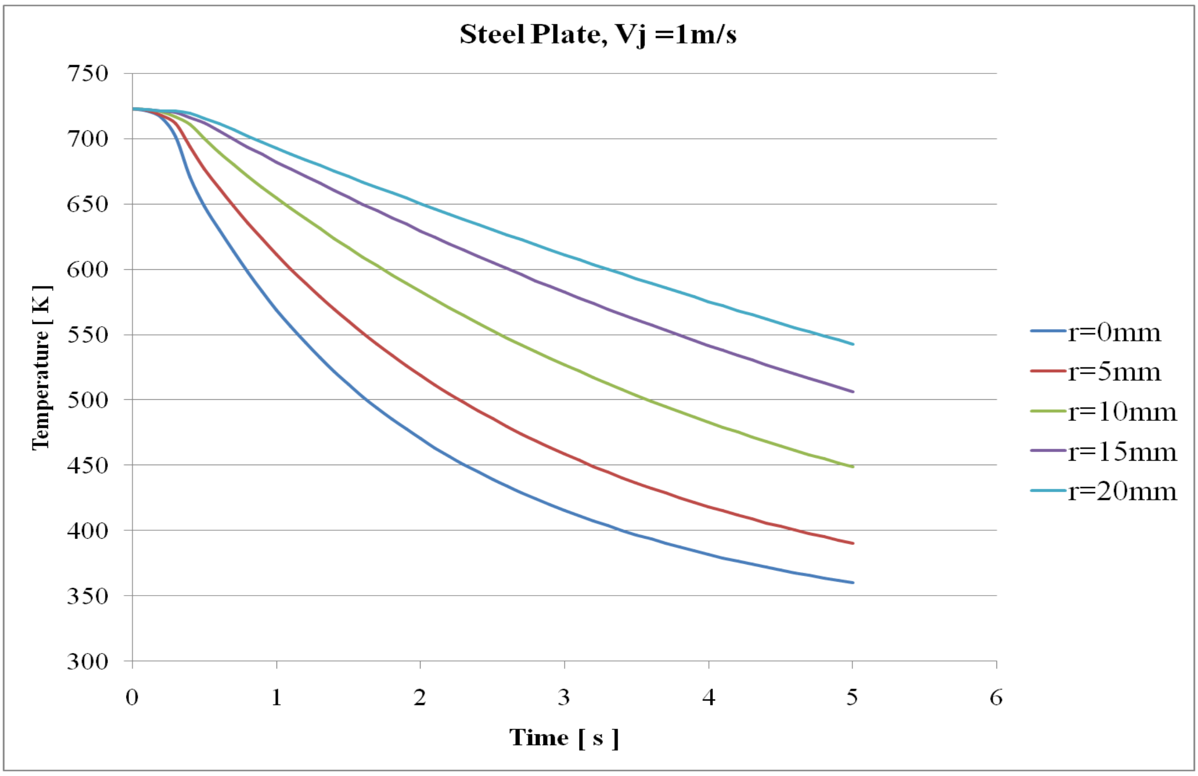

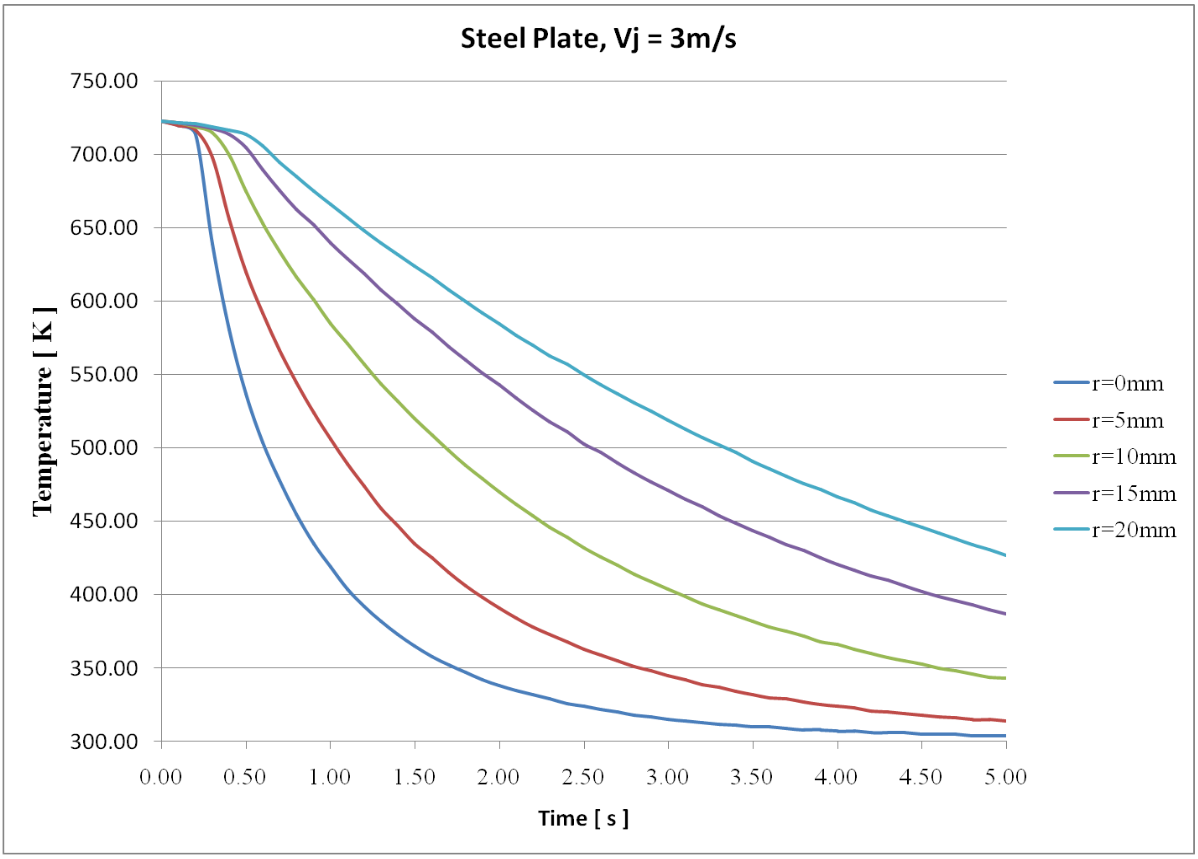

Table 1 : Observation on Steel Plate

S.No	Vj	CHF (MW/m^2)	Temperature after 5s [K]
1	1m/s	0.879723	360.0824
2	3m/s	2.212670	304.00

7.2. Aluminium Plate

Wall heat fluxes Plots

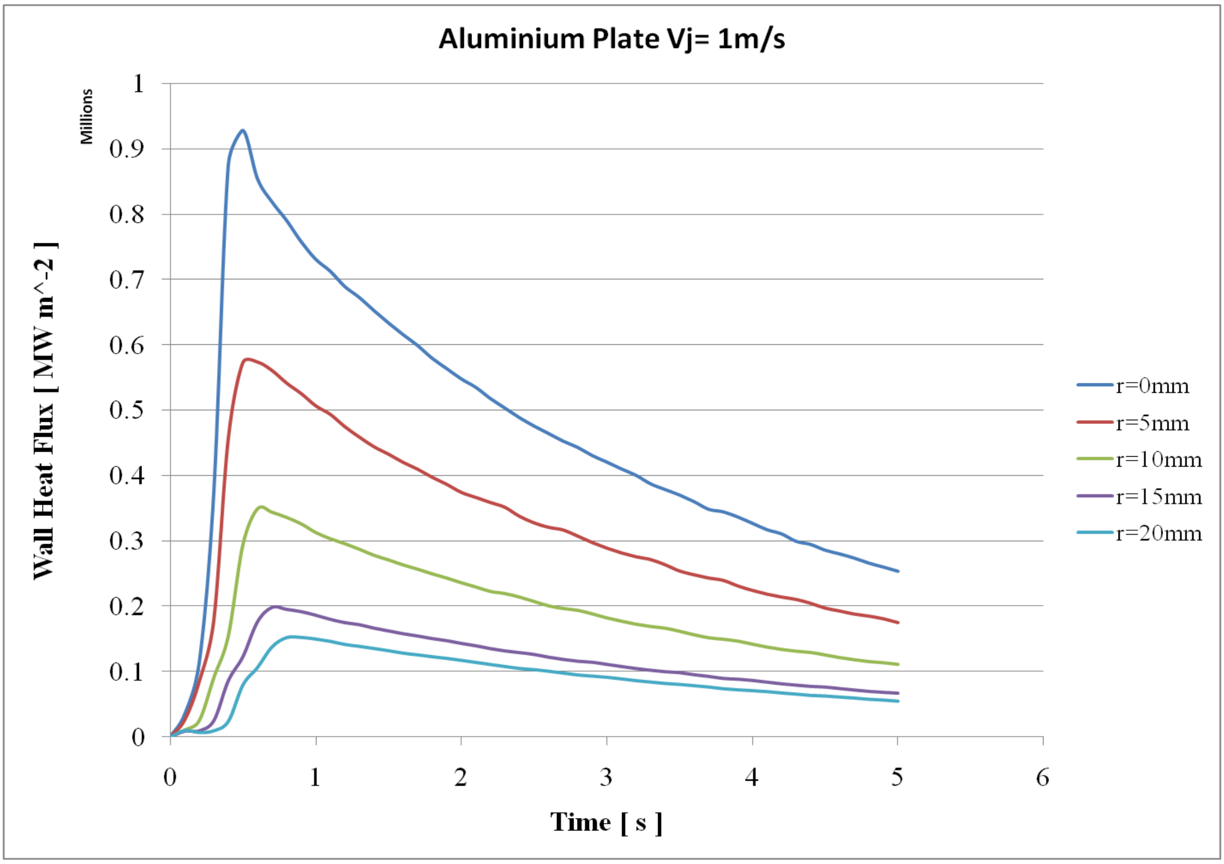

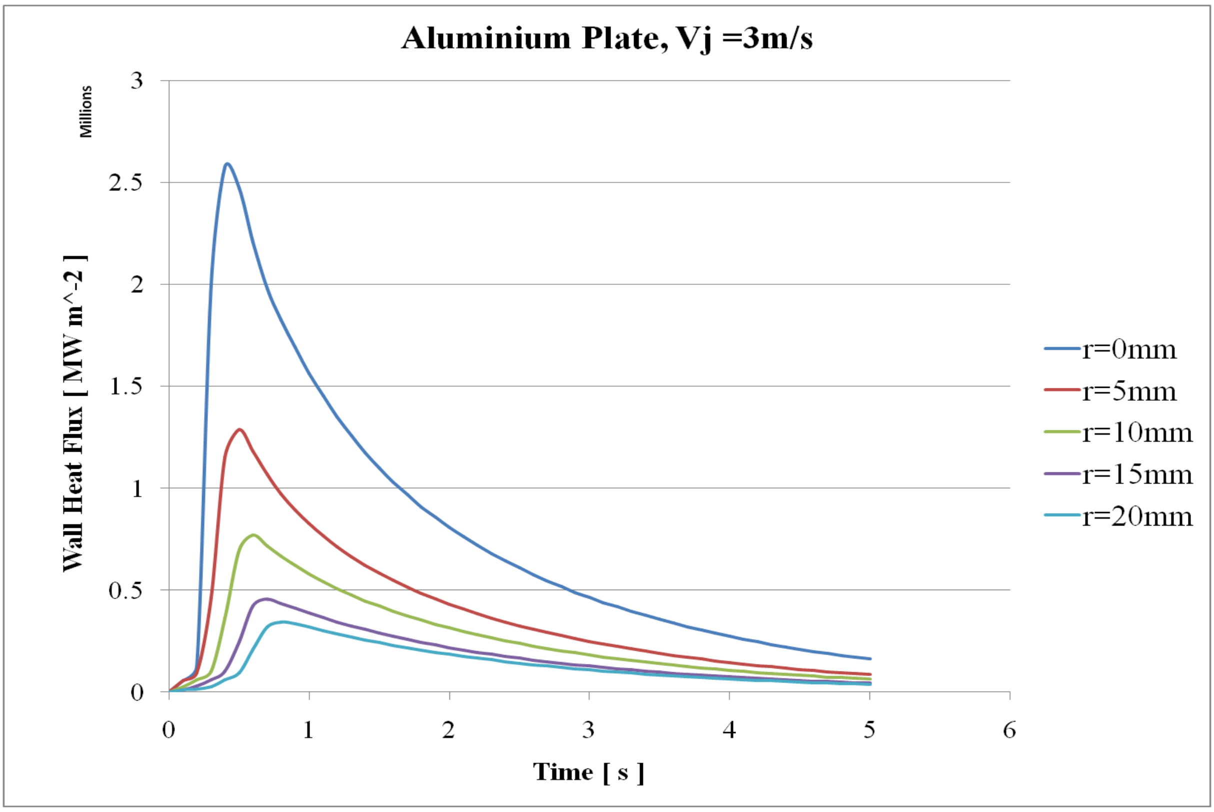
Aluminium Plate, Vj =3m/s
Millions
Wall Heat Flux [MW m^-2]
3
2.5
2
1.5
1
0.5
0
0
1
2
3
4
5
6
Time [s]
r=0mm
r=5mm
r=10mm
r=15mm
r=20mm

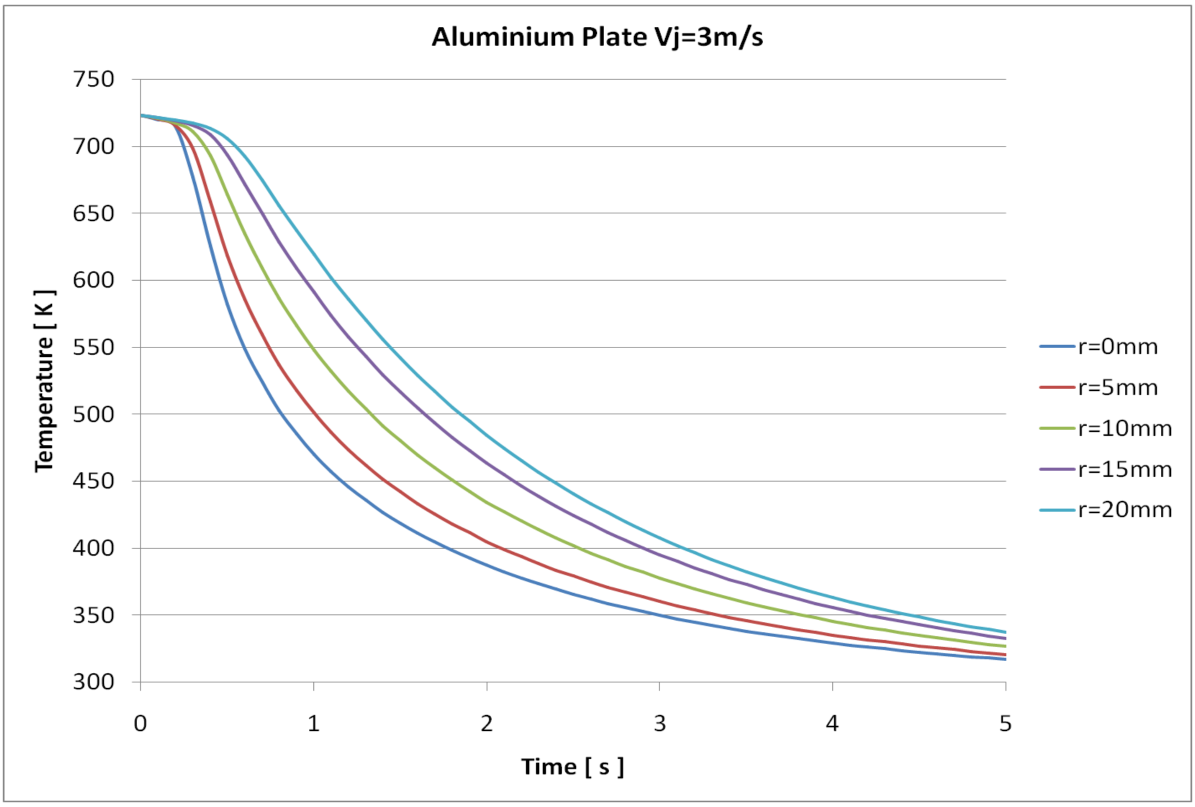
Aluminium Plate Vj=3m/s
Temperature [K]
750
700
650
600
550
500
450
400
350
300
0
1
2
3
4
5
Time [s]
r=0mm
r=5mm
r=10mm
r=15mm
r=20mm

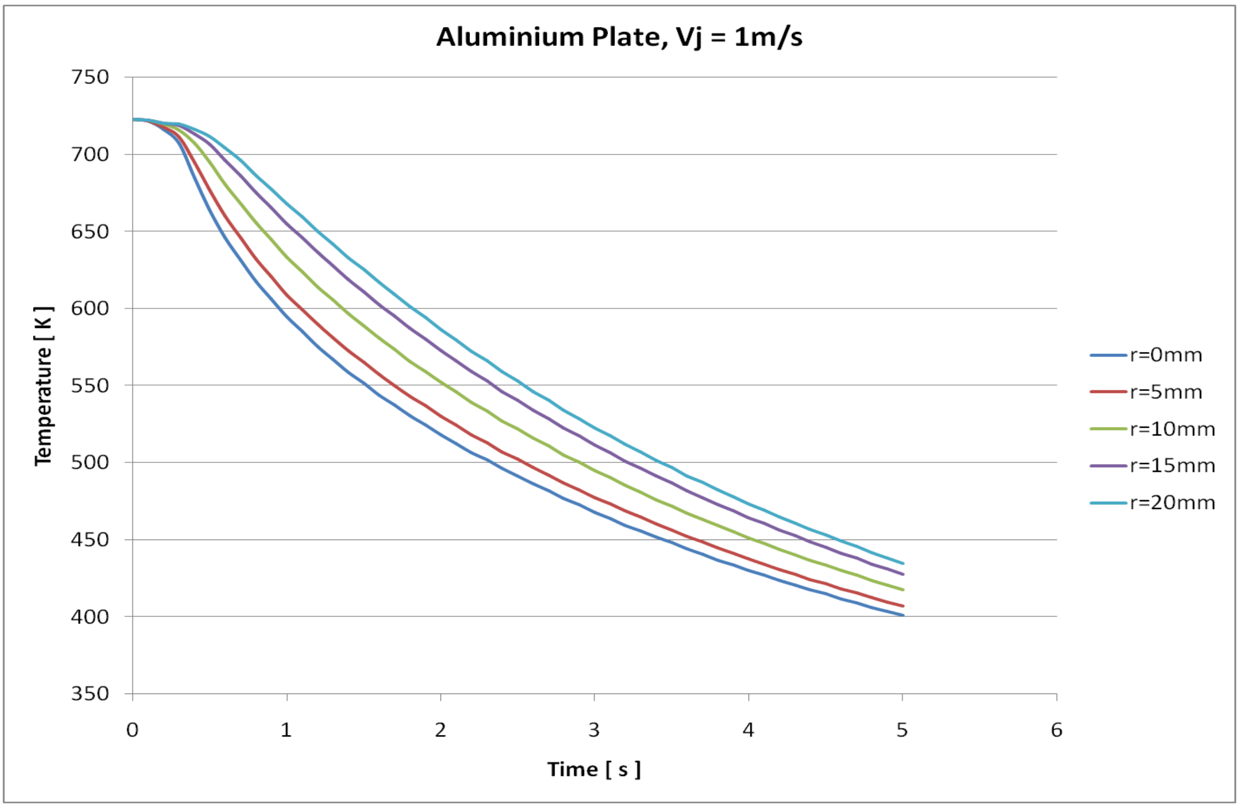

Table 2 Observation on Aluminium Plate

S.No.	V_j	CHF (MW/m^2)	Temperature after 5s
1	1m/s	0.928532	401.0086
2	3m/s	2.574102	317.1184

We can see from all plots and all tables by increasing jet velocity, the critical wall heat flux value is also increased by some extent but not proportionally to the change in velocity. The reason behind not getting proportional change is due splashing of the liquid at high velocity which impact the total heat transfer rate of the plate.

7.3. Temperature Contours at different time

<table>
<tr><th>Time, t(s)</th><th>Steel Plate Vj= 1m/.s</th><th>Steel Plate Vj= 3m/.s</th></tr>
<tr><td>t=0</td><td>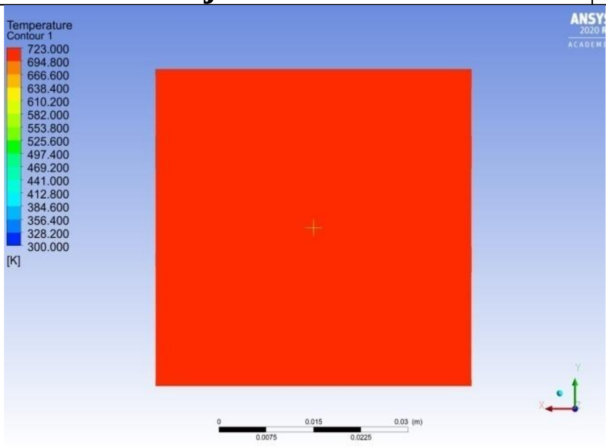
</td><td>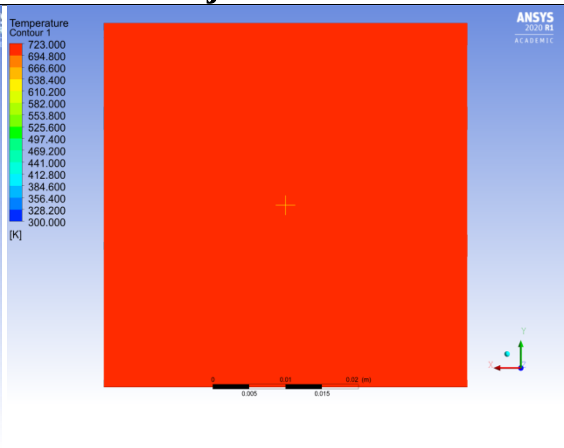
</td></tr>
<tr><td>t=5</td><td>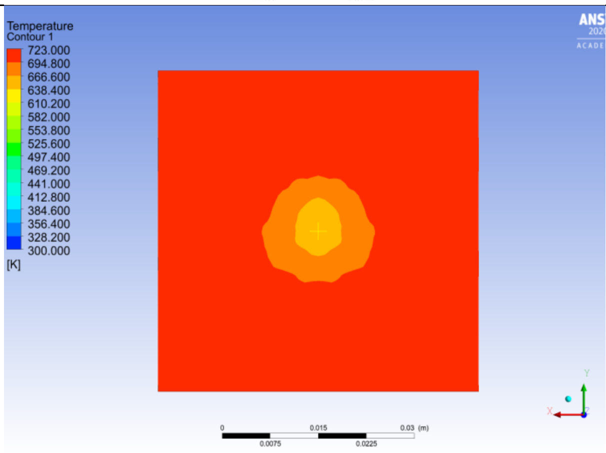
</td><td>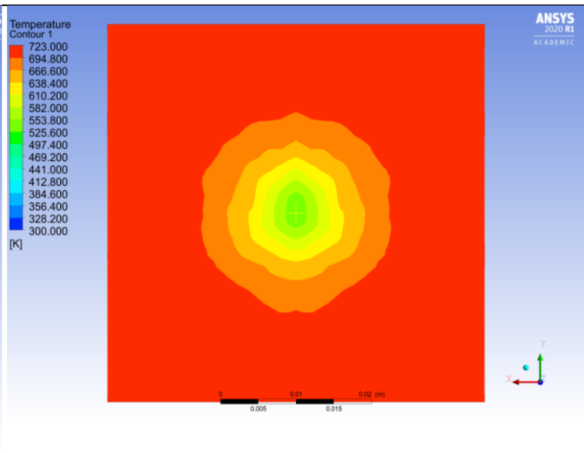
</td></tr>
<tr><td>t=20</td><td>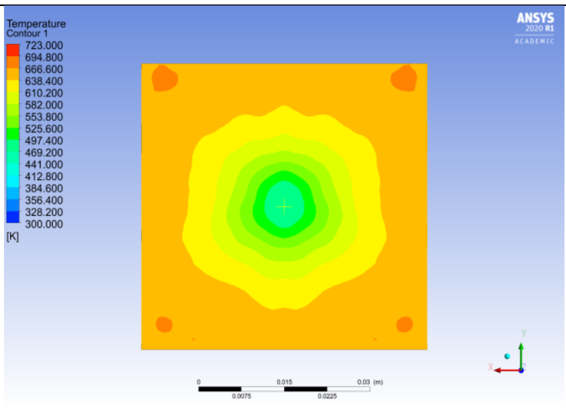
</td><td>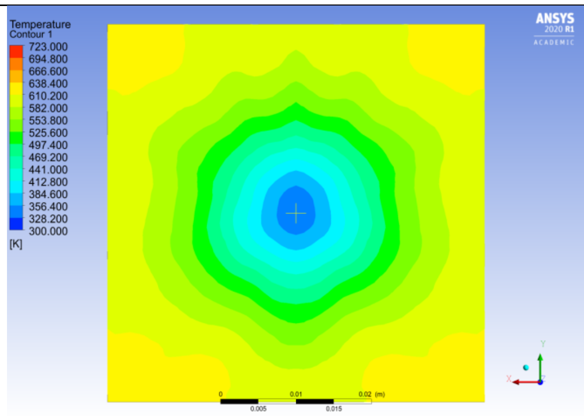
</td></tr>
<tr><td>t=50</td><td>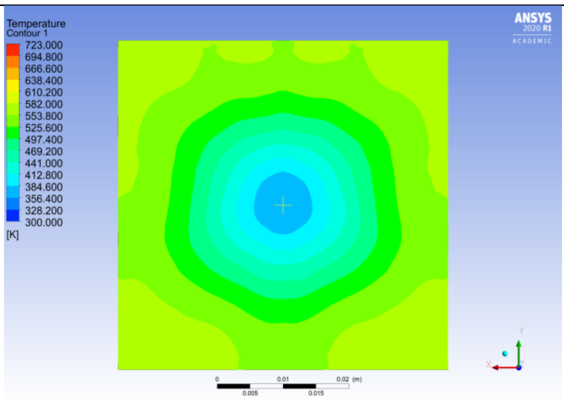
</td><td>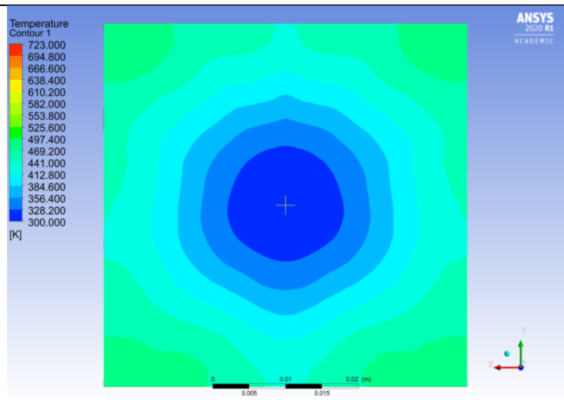
</td></tr>
</table>

<table>
<tr><th>Time, t (s)</th><th>Aluminium Plate Vj= 1m/.s</th><th>Aluminium Plate Vj= 3m/.s</th></tr>
<tr><td>t=0</td><td>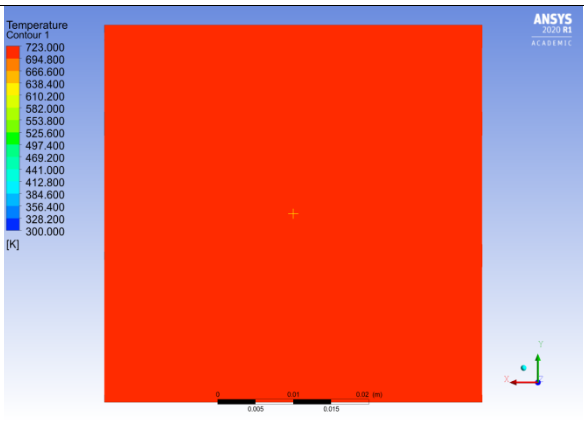
</td><td>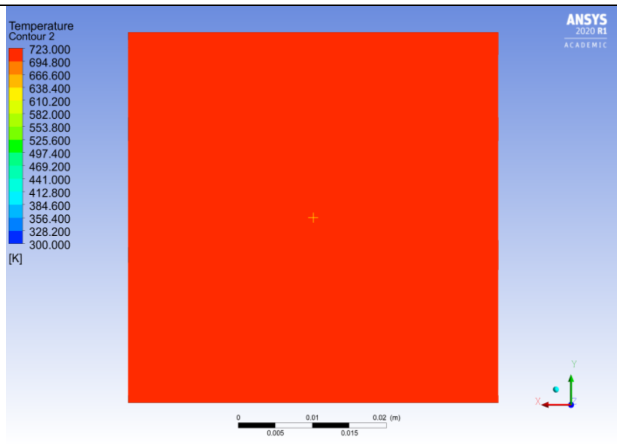
</td></tr>
<tr><td>t=5</td><td>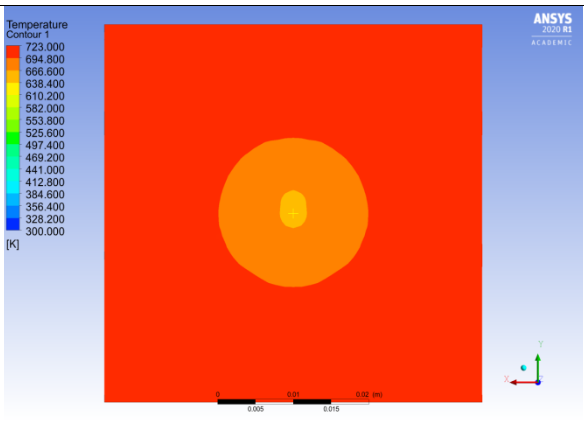
</td><td>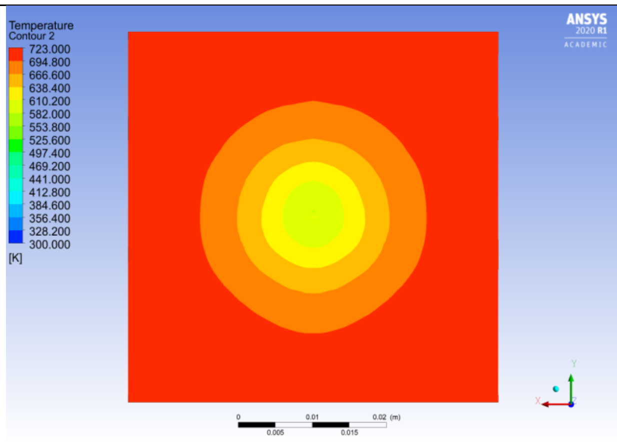
</td></tr>
<tr><td>t=20</td><td>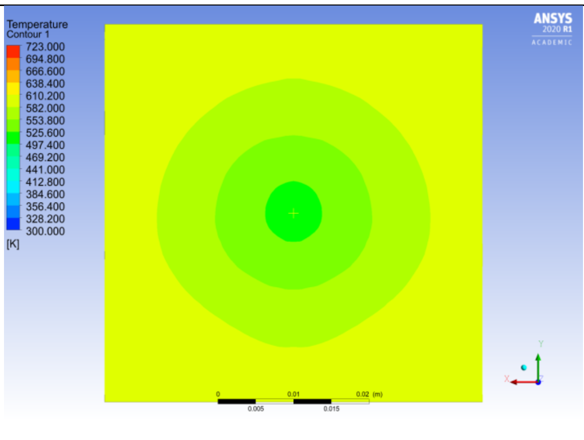
</td><td>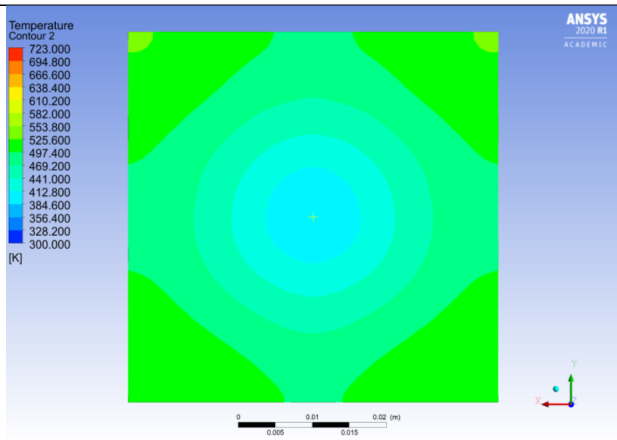
</td></tr>
<tr><td>t=50</td><td>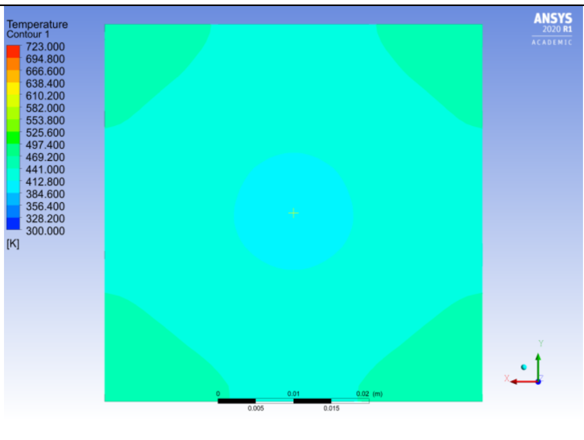
</td><td>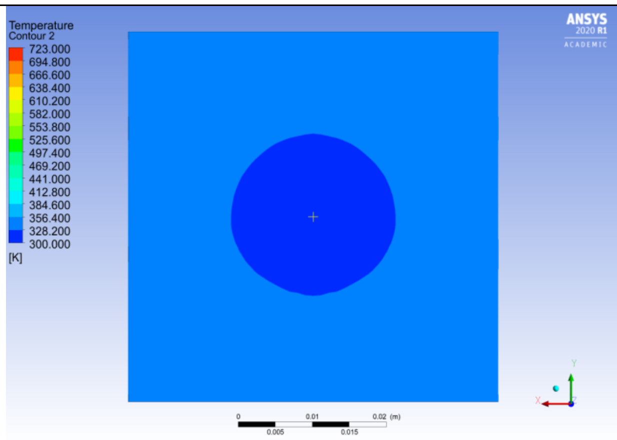
</td></tr>
</table>

7.4. Comparison between Aluminium plate and Steel Plate

Table 3 Comparison between Steel and Aluminium

S.No	Plate Material	V_j	CHF(MW/m^{2})	Temperature after 5s [K]
1	Steel	1m/s	0.879723	360.0824
	Al	1m/s	0.928532.8	401.0086
2	Steel	3m/s	2.212670	304.00
	Al	3m/s	2.574102	317.1184

Here we are getting very interesting results for steel and aluminium plate cooling rate is more in case of steel than Al and get higher wall heat flux value for Aluminium. So we can conclude that Aluminium gives higher resistance to the wetting front of water impingement than steel plate.

This because of Al have higher thermal conductivity than steel so the film boiling carried out in the case of Al is more than steel.

CHAPTER 8

Conclusions and Recommendation

The results of the numerical solution can be summarised as follows:

1. Quenching temperature drop in the radial direction for lower Reynolds numbers is greater in comparison to higher Reynolds numbers.

2. By increasing the time and the movement towards flow downstream, wetting front grows, and by increasing the velocity of the fluid jet, radius of the wetting zone also increases. In fact, by increasing quenching velocity, the movement of the wetting front towards flow downstream zone occurs sooner and the growth of wetting zone expands faster, and by increasing the velocity radius of the wetting zone occurs very fast.

3. By increasing the radius of the wetting zone towards the flow downstream, the heat flux increases and the surface temperature decreases

4. By increasing the velocity of the fluid jet at a constant sub- cooling temperature, cooling rate increases. More ever, by increasing the velocity of the fluid jet, the elapsed time for transition from film boiling to nucleate boiling occurs faster

5. The maximum amount of heat flux occurs at the stagnation point, and after that near the stagnation point, it appears for less radial positions.

The extension of this research work according to our recent work for nanofluids jet impingement affords engineers a good option for turbulent jet simulation.

References

A. K. Mozumder, M. Monde, P. L. Woodfield, M. A. Islam, Int. J. Heat Mass Transfer 2006, 49, 2877.

C. Agarwal, R. Kumar, A. Gupta, B. Chatterjee, Exp. Heat Transfer 2014, 27, 256.

C. Agarwal, R. Kumar, A. Gupta, B. Chatterjee, Nucl. Eng. Des. 2013, 265, 727.

C. Agrawal, D. Gotherwal, C. D. Singh, C. Singh, Heat Mass Transfer 2017, 53, 733.

C. Agrawal, R. Kumar, A. Gupta, B. Chatterjee, Exp. Therm. Fluid Sci. 2012, 42, 25.

C. Agrawal, R. Kumar, A. Gupta, B. Chatterjee, Heat Mass Transfer 2016, 52, 1203.

C. Agrawal, R. Kumar, A. Gupta, B. Chatterjee, Heat Transfer Eng. 2017, 38, 1209.

C. Agrawal, R. Kumar, A. Gupta, B. Chatterjee, Int. J. Heat Mass Transfer 2012, 55, 4772.

C. Agrawal, R. Kumar, A. Gupta, B. Chatterjee, Int. J. Therm. Sci. 2013, 71, 310.

C. Agrawal, R. Kumar, A. Gupta, B. Chatterjee, J. Enhanced Heat Transfer 2015, 22, 199.

C. Agrawal, R. Kumar, A. Gupta, B. Chatterjee, J. Therm. Anal. Calorim. 2016, 123, 861.

C. Agrawal, R. Kumar, A. Gupta, B. Chatterjee, Trans. ASME Therm. Sci. Eng. Appl. 2013, 5, 011007.

N. Karwa, T. G. Roisman, P. Stephan, C. Tropea, Int. J. Therm. Sci. 2011, 50, 993.

Q. Xie, B. Wang, Y. Wang, Z. Wang, G. Wang, ISIJ Int. 2016, 56,1210

T. Ochi, S. Nakanishi, M. Kaji, S. Ishigai, 3rd Multi-phase Flow and Heat Transfer Symposium-Workshop, Miami Beach, Florida, USA. 18–20 April, 1983.

V. Koldin, N. I. Platonov, Therm. Eng. 2008, 55, 223.

Z. H. Liu, T. F. Tong, Y. H. Qiu, ASME J. Heat Transfer 2004, 126, 179.